bioRxiv preprint doi: https://doi.org/10.1101/2024.01.07.574580; this version posted January 8, 2024. The copyright holder for this preprint (which was not certified by peer review) is the author/funder, who has granted bioRxiv a license to display the preprint in perpetuity. It is made available under aCC-BY 4.0 International license.

Epstein-Barr virus protein EBNA-LP engages YY1 through leucine-rich motifs to promote naïve B cell transformation

Jana M Cable[1], Nicolás M Reinoso-Vizcaino[1], Robert E. White[2], Micah A Luftig[1*]

[1] Department of Molecular Genetics and Microbiology, Duke University School of Medicine, Durham, NC, United States

[2] Section of Virology, Department of Infectious Disease, Imperial College London, London, United Kingdom

*Corresponding author

Email: micah.luftig@duke.edu

bioRxiv preprint doi: https://doi.org/10.1101/2024.01.07.574580; this version posted January 8, 2024. The copyright holder for this preprint (which was not certified by peer review) is the author/funder, who has granted bioRxiv a license to display the preprint in perpetuity. It is made available under aCC-BY 4.0 International license.

Abstract

Epstein-Barr Virus (EBV) is associated with numerous cancers including B cell lymphomas. *In vitro*, EBV transforms primary B cells into immortalized Lymphoblastoid Cell Lines (LCLs) which serves as a model to study the role of viral proteins in EBV malignancies. EBV induced cellular transformation is driven by viral proteins including EBV-Nuclear Antigens (EBNAs). EBNA-LP is important for the transformation of naïve but not memory B cells. While EBNA-LP was thought to promote gene activation by EBNA2, EBNA-LP Knock Out (LPKO) virus-infected cells express EBNA2-activated genes efficiently. Therefore, a gap in knowledge exists as to what roles EBNA-LP plays in naïve B cell transformation. We developed a trans-complementation assay wherein transfection with wild-type EBNA-LP rescues the transformation of peripheral blood- and cord blood-derived naïve B cells by LPKO virus. Despite EBNA-LP phosphorylation sites being important in EBNA2 co-activation; neither phospho-mutant nor phospho-mimetic EBNA-LP was defective in rescuing naïve B cell outgrowth. However, we identified conserved leucine-rich motifs in EBNA-LP that were required for transformation of adult naïve and cord blood B cells. Because cellular PPAR-γ coactivator (PGC) proteins use leucine-rich motifs to engage transcription factors including YY1, a key regulator of DNA looping and metabolism, we examined the role of EBNA-LP in engaging cellular transcription factors. We found a significant overlap between EBNA-LP and YY1 in ChIP-Seq data and confirmed their biochemical association in LCLs by endogenous co-immunoprecipitation. Moreover, we found that the EBNA-LP leucine-rich motifs were required for YY1 interaction in LCLs. Finally, we used Cas9 to knockout YY1 in primary total B cells and naïve B cells prior to EBV infection and found YY1 to be essential for EBV-mediated transformation. We propose that EBNA-LP engages YY1 through conserved leucine-rich motifs to promote EBV transformation of naïve B cells.

Author Summary

Epstein-Barr Virus (EBV) is associated with various B cell lymphomas, particularly in immunosuppressed individuals. In the absence of a functional immune system, viral latency proteins, including EBV Nuclear Antigens (EBNAs) act as oncoproteins to promote tumorigenesis. EBNA-LP is one of the first viral proteins produced after infection and is important for the transformation of naïve B cells. However, the roles of EBNA-LP during infection are largely undefined. In this study, developed an assay in which the role of wild type and mutant EBNA-LP could be investigated

bioRxiv preprint doi: https://doi.org/10.1101/2024.01.07.574580; this version posted January 8, 2024. The copyright holder for this preprint (which was not certified by peer review) is the author/funder, who has granted bioRxiv a license to display the preprint in perpetuity. It is made available under aCC-BY 4.0 International license.

in context of primary naïve B cells infected with an EBNA-LP Knock Out virus. Using this assay, we identified highly conserved leucine-rich motifs within EBNA-LP that are important for transformation of EBV-infected naïve B cells. These conserved motifs associate with the cellular transcription factor YY1, an important transcriptional regulator in B cell development and in many cancers, that we now show is essential for outgrowth of EBV infected B cells. Our study provides further insights into the mechanisms by which EBV transforms naïve B cells.

Introduction

Epstein-Barr virus (EBV) is a gamma-herpesvirus that infects – and permanently resides in – nearly all individuals by adulthood. EBV infects resting B cells, which leads to B cell activation followed by a life-long latent infection in memory B cells [1]. While infection is typically asymptomatic, EBV is associated with numerous malignancies including B cell lymphomas such as Hodgkin's Lymphoma, Burkitt Lymphoma, and lymphoproliferative disease in immunocompromised individuals [2]. EBV-induced cellular proliferation is largely driven by the activity of viral proteins.

EBV infection of B cells leads to the expression of the viral latency program which includes EBV Nuclear Antigens (EBNAs) and Latent Membrane Protein (LMPs). EBNAs are transcriptional regulators which include EBNA1, 2, 3A, 3B, 3C, and -Leader Protein (LP). Other than EBNA1, the EBNA proteins do not directly bind DNA, but rather regulate transcription by engaging with cellular DNA sequence-specific binding proteins. EBNA2 and EBNA-LP are the initial viral latency proteins expressed, being detected as early as 12 hours post infection from the repeated viral W promoter (Wp) [3-5]. Once EBNA2 and EBNA-LP are expressed, the C promoter (Cp) becomes transcriptionally active from which promoter EBNAs are then predominantly transcribed, followed by the LMP proteins which take 1-2 weeks to reach the level sustained in LCLs [5, 6]. *In vitro*, infected cells initially increase in size, followed by a phase of cellular hyperproliferation beginning 3-4 days post infection, followed by a slower period of cellular outgrowth [7]. Restriction by innate cellular barriers including metabolic stress and DNA damage ultimately leads to cellular arrest of many infected cells [8]. However, cells that overcome these barriers *in vitro* are transformed into immortalized lymphoblastoid cell lines (LCLs), serving as a model to study the role of viral proteins in primary B cell infection and EBV-associated malignancies.

bioRxiv preprint doi: https://doi.org/10.1101/2024.01.07.574580; this version posted January 8, 2024. The copyright holder for this preprint (which was not certified by peer review) is the author/funder, who has granted bioRxiv a license to display the preprint in perpetuity. It is made available under aCC-BY 4.0 International license.

EBNA2 is an important regulator of both viral and cellular genes and is required at all stages of primary infection *in vitro* [9]. Importantly, EBNA2 engages several host transcription factors including RBPJ and EBF1 to induce high levels of the oncogene Myc, among other cellular genes [10-12]. While less is known about the role of EBNA-LP in EBV infection and cellular transformation, several studies have contributed to our knowledge of EBNA-LP activity in infected B cells. The main function of EBNA-LP has been ascribed to co-activating EBNA2 activity at both viral and host genes. In transfection experiments performed outside of the context of primary infection, EBNA-LP increases EBNA2 activation of the Cp, LMP1 promoter, RBPJ-binding sites, and cellular genes including HES1 [13-15]. However, studies identifying which domains of EBNA-LP are responsible for this activity have found conflicting results [13-15]. EBNA-LP is also hypothesized to promote EBNA2 activity by removing transcriptional repressors including NCoR and HA95 from EBNA2 targeted sites [15-17]. EBNA-LP enriched sites on chromatin are also associated with several cellular transcription factors and DNA looping factors [15-18]. Furthermore, upon B cell infection and in LCLs, EBNA-LP localizes to the subnuclear foci called PML bodies, which are implicated in restricting viral gene expression [19, 20]. However, the significance of these many EBNA-LP functions in the context of primary infection are still unclear.

The N-terminal part of EBNA-LP is composed of variable numbers of repeats of a 66 amino acid domain (encoded by W1 and W2 exons within the major internal repeat of the EBV genome, which we will call the W domain), and its C-terminus (called the Y domain, as it derives from exons Y1 and Y2) contains 45 amino acids. Circulating viruses encode at least 4 repeated W domains [21]. Alternative Wp usage and splicing leads to expression of multiple EBNA-LP isoforms with variable numbers of W domains. Across the W and Y domains, there are five evolutionarily conserved regions (CR) between EBV EBNA-LP and its homologs in primate lymphocryptovirus (LCV) [22]. One study found that all three conserved regions in the W domain (CR1, CR2, CR3) are required to enhance the activation of genes by EBNA2, while motifs within CR1 and CR2 contain a bi-partite nuclear localization signal [22-24]. The Y domain contains two additional conserved regions (CR4 and CR5) [22]. Importantly, the significance of the conserved regions has not been studied in the context of primary infection.

In addition to these conserved regions, EBNA-LP also contains several phosphorylated serine residues in the W domain. One of which, serine 36 (S36), is highly conserved across EBNA-LP homologs in lymphocryptovirus [23, 25-27]. Serine 34 (S34) and 63 (S63), in CR3, are also possible sites of phosphorylation, although to date

bioRxiv preprint doi: https://doi.org/10.1101/2024.01.07.574580; this version posted January 8, 2024. The copyright holder for this preprint (which was not certified by peer review) is the author/funder, who has granted bioRxiv a license to display the preprint in perpetuity. It is made available under aCC-BY 4.0 International license.

96 modification at S34 and S63 has not been validated [24]. EBNA-LP can be phosphorylated in a cell cycle-dependent
97 manner by numerous kinases including Casein Kinase II, $p34^{cdc2}$, DNA-PK, and the viral kinase BGLF4, with EBNA-
98 LP being most highly phosphorylated during G_2 [24, 27-30]. In transfection assays, phosphorylation of EBNA-LP is
99 required for its ability to help EBNA2 to induce Cp and LMP1 transcription [23, 24, 29]. Phosphorylation of EBNA-LP
100 is also required for its association with the histone acetyltransferase p300 [31].

101 EBNA-LP is essential in transforming cord blood-derived B cells which are exclusively naïve, and is
102 significantly more important for transformation of sorted adult peripheral blood naïve B cells, defined as IgD+/CD27,
103 than adult peripheral blood memory B cells [32]. A similar study in adenoid tissue-derived naïve B cells found EBNA-
104 LP was critical during early stages of infection for cell division and survival [9]. In the absence of the EBNA-LP Y
105 domain, the efficiency of cellular transformation of infected B cells is significantly reduced [33, 34]. While the function
106 of the Y domain is unknown, leucines in the Y domain CR4 have been implicated as the site of interaction with the
107 transcription factor Estrogen Related Receptor Alpha (ERRα) [35]. Intriguingly, ERRα is a transcription factor that is
108 co-activated by the Peroxisome PPAR-γ Coactivator (PGC) family of proteins [36]. The PGC proteins, like many other
109 transcriptional co-activators, utilize their leucine-rich motifs (LRMS) typically of the sequence LXXLL to bind
110 transcription factors and then recruit additional co-activators to promote transcription [36-38]. We therefore sought to
111 determine whether the LRMs within EBNA-LP could be important motifs functionally mimicking the LRMs in cellular
112 PGC co-activators of transcription.

113 Despite the proposed role of EBNA-LP in assisting EBNA2-mediated transcriptional activation, genetic
114 studies with an EBNA-LP knock out (LPKO) virus indicates EBNA-LP is in fact not required for EBNA2 to activate
115 host genes including Myc, nor for EBNA2 recruitment to cellular chromatin [32], but rather may constrain excessive
116 EBNA2-mediated activation of cellular genes. Therefore, we sought to uncover other important roles of EBNA-LP in
117 EBV-infected B cells in a physiologically relevant context. To do so, we used a trans-complementation assay to define
118 the importance of conserved regions and posttranslational modifications of EBNA-LP in the transformation of naïve
119 B cells by EBV.

bioRxiv preprint doi: https://doi.org/10.1101/2024.01.07.574580; this version posted January 8, 2024. The copyright holder for this preprint (which was not certified by peer review) is the author/funder, who has granted bioRxiv a license to display the preprint in perpetuity. It is made available under aCC-BY 4.0 International license.

Results

Naïve B Cells Infected with LPKO Virus are Rescued by Trans-Complementation with Wild-Type EBNA-LP

In order to assay the consequences of EBNA-LP mutations, we developed a trans-complementation assay. First, we tested whether outgrowth of adult naïve B cells infected with EBNA-LP Knock Out (LPKO) virus could be rescued by expression of exogenous, wild type EBNA-LP**.** We created a complementation vector encoding FLAG-tdTomato, a P2A cleavage site, wild type FLAG-EBNA-LP including four of the repeated W domains codon optimized to improve plasmid stability (S1 Table), and the EBV oriP and EBNA1 to allow episomal persistence of the vector (S1A-B Fig). Naïve B cells derived from adult peripheral blood mononuclear cells (PBMCs) were isolated by immunomagnetic selection for IgD+/CD27- cells, although purity varied by donor ranging from 92.2-97.6% with the majority of contaminating cells coming from IgD-/CD27- B cells, highlighting the challenges of isolating pure naïve B cell from adult PBMCs (S2A Fig). For each replicate, isolated cells were transfected with the complementation vector encoding EBNA-LP, with vector encoding only FLAG-tdTomato, or left untransfected (Fig 1A). Cells were then infected with LPKO or WT virus [32] at a titer determined to infect almost 100% of cells. Outgrowth of tdTomato positive cells, indicative of maintenance of the episomal vector, was then assayed by flow cytometry every seven days post transfection, with compensation for GFP produced by the virus (S2B Fig). While the electroporation of primary B cells resulted in killing of some transfected cells, the similarity in total proliferating cells between untransfected cells and cells transfected with only vector for WT-infected cells indicated that the failure of LPKO-infected cells transfected with vector to proliferate was not a result of electroporation, but rather reflects the importance of EBNA-LP early during infection in peripheral blood-derived naïve B cells (S2C, S2D Fig).

In all three adult blood donors, trans-complementation of naïve B cells with EBNA-LP that were infected with LPKO virus led to outgrowth of tdTomato positive cells over time similar to WT virus infected cells transfected with the tdTomato vector lacking EBNA-LP (Fig 1B). Of note, there was a high degree of variability in outgrowth efficiency between replicates both within and between donors. LPKO infected cells transfected with vector encoding only tdTomato consistently failed to expand tdTomato positive cells, whereas trans-complementation with EBNA-LP

bioRxiv preprint doi: https://doi.org/10.1101/2024.01.07.574580; this version posted January 8, 2024. The copyright holder for this preprint (which was not certified by peer review) is the author/funder, who has granted bioRxiv a license to display the preprint in perpetuity. It is made available under aCC-BY 4.0 International license.

rescued outgrowth and successfully generated tdTomato+ LCLs (Fig 1C-1E). As expected, WT virus transformed untransfected naïve B cells into tdTomato negative LCLs in each replicate across three donors (Fig 1E). WT infected cells transfected with vector also generated LCLs and retained tdTomato expression, albeit only in a small proportion – on average fewer than 3% – of cells (S2E Fig). As the purified naïve B cell populations still contain contaminating unconventional memory B cells (IgD-/CD27-), which do not require EBNA-LP for outgrowth and cellular transformation [32, 39] (S2A Fig), tdTomato negative LCLs were observed following LPKO infection in both untransfected and cells trans-complemented with only tdTomato in some donors (Fig 1E, S2E Fig). Rescued LCLs retained EBNA-LP expression at levels comparable to WT LCLs (Fig. 1F). The ability of this trans-complementation assay to consistently rescue transformation of LPKO infected naïve B cells and retain EBNA-LP expression confirms this assay can also be used to assess the role of EBNA-LP mutants in the context of primary infection.

Phosphorylation of EBNA-LP is not Required for Naïve B Cell Transformation

Phosphorylation of EBNA-LP is considered essential for EBNA-LP-mediated coactivation of EBNA2 [23, 24, 29]. Therefore, we sought to uncover whether phosphorylation is required for EBNA-LP-mediated transformation of naïve B cells. All three predicted phosphorylated serines (S34, S36, and S63) are conserved across EBV Type 1 and Type 2 strains, while S36 is also conserved across EBV strains and in strains of the non-human primate lymphocryptovirus (LCV), the closest common ancestor to EBV [22, 24] (Fig 2A). We assessed phosphorylation of EBNA-LP by performing FLAG immunoprecipitation followed by mass spectrometry with trypsin digestion of our FLAG-tagged EBNA-LP encoding 4 W domains expressed in 293T cells. In total, 81 peptides were identified which covered most of the EBNA-LP protein (Fig 2B). Only two peptides spanning S34 and S36 were identified, likely because they are located in a region rich in arginine, the site of trypsin cleavage (Fig 2B) [40, 41]. However, of these identified peptides, one contained phosphorylated S34 (32-HRSpPSPTR-39) (Fig 2C and S3A Fig) and the other phosphorylated S36, (34-SPSpPTRGGQEPR-45) suggesting phosphorylation is a highly abundant modification at S34 and S36 (Fig 2C and S3B Fig). Peptides spanning S63 were also identified (including 51-VLVQQEEEVVSGSpPSGPR-68) (S3C Fig) with phosphorylation at S63 observed in 6 out of 41 peptides (Fig 2C**).**

bioRxiv preprint doi: https://doi.org/10.1101/2024.01.07.574580; this version posted January 8, 2024. The copyright holder for this preprint (which was not certified by peer review) is the author/funder, who has granted bioRxiv a license to display the preprint in perpetuity. It is made available under aCC-BY 4.0 International license.

While phosphorylation of S36 has previously been confirmed, this is the first study to validate S34 and S63 as phosphorylation sites on EBNA-LP by mass spectrometry.

We then generated both a FLAG-tagged phospho-mutant (S3A) in which S34, S36, and S63 were modified to alanine, and a phospho-mimetic (S3E) in which S34, S36, and S63 were modified to glutamic acid. Wild Type, S3A, and S3E EBNA-LP were transfected into 293T cells, and FLAG immunoprecipitations to enrich for EBNA-LP were performed in triplicate for each construct prior to analysis by mass spectrometry using Tandem Mass Tag (TMT) labelling to quantify the signal of identified peptides across samples. Only wild type EBNA-LP was phosphorylated, with peptides containing phospho-residue S63, but no phosphorylated peptides were detected from either EBNA-LP-S3A or -S3E (Fig 2D), although no peptides covering S34 and S36 were identified in this experiment. This confirms S34, S36, and S63 as the only sites of phosphorylation on EBNA-LP, further validating that other highly conserved serines including S61 are not phosphorylated.

We then tested whether EBNA-LP-S3A or -S3E could rescue LPKO virus infected naïve B cells. Despite the previously inferred importance of EBNA-LP phosphorylation sites, we found that, surprisingly, trans-complementation with either the phospho-mutant or phospho-mimetic could rescue LPKO infected naïve B cells to the same degree as wild-type EBNA-LP both 14 days post infection (Fig 2E) and 28-35 days post infection (Fig 2F). Both mutants also successfully generated tdTomato positive LCLs similar to wild type EBNA-LP (Fig 2G). Further, EBNA-LP-S3A and -S3E constructs were retained and expressed EBNA-LP protein in trans-complemented LCLs (Fig 2H). These findings suggest that the EBNA2 co-activation assay may not faithfully recapitulate the functions important for EBNA-LP in naïve B cell transformation.

EBNA-LP Contains Conserved, Leucine-Rich Motifs that are Essential for Naïve B Cell Transformation

Since the sites of EBNA-LP phosphorylation are non-essential for transformation of naïve B cells, we next sought to determine what other motifs in EBNA-LP could be important for mediating naïve B cell transformation. We identified highly conserved leucine-rich motifs (LRM) in both the repeated W domain CR1s and Y domain CR4 [22, 35] (Fig 3A). Because these motifs are reminiscent of the leucine-rich motifs in the PGC coactivator family, we hypothesized that these conserved regions could be important for mediating EBNA-LP interaction with cellular factors.

bioRxiv preprint doi: https://doi.org/10.1101/2024.01.07.574580; this version posted January 8, 2024. The copyright holder for this preprint (which was not certified by peer review) is the author/funder, who has granted bioRxiv a license to display the preprint in perpetuity. It is made available under aCC-BY 4.0 International license.

We therefore generated constructs in which the leucines in LRMs of both the W domain CR1s and Y domain CR4 were mutated to alanine (LRM mutant) (Fig 3B). At 14 days post infection, there were significantly fewer tdTomato positive cells in the LPKO virus infected cells trans-complemented with the LRM Mutant compared to trans-complementation with wild type EBNA-LP (Fig 3C). At this early time point there was also a higher total number of cells in LPKO virus rescued by wild type EBNA-LP compared to the LRM Mutant (S4A Fig), further supporting the inability of the LRM mutant to rescue LPKO virus early during infection. Trans-complementation with wild type EBNA-LP continued to promote higher outgrowth of tdTomato positive cells compared to the LRM mutant 28-35 days post infection (Fig 3D), and the LRM mutant failed to generate tdTomato positive LCLs from LPKO infected adult naïve B cells (Fig 3E). We did, however, observe rare outgrowth of tdTomato negative LCLs in all donors as even a small level of contaminating memory cells could ultimately take over the culture during weeks of B cell outgrowth (Fig 3E, S4B and S4C Fig).

As cord blood provides a purer naïve B cell population [42], we next assessed the ability of the LRM mutant to rescue LPKO infected cord blood B cells. Like adult naïve B cells, the cord blood B cells could support outgrowth of rescued, tdTomato-positive cells over time (Fig 4A and 4B) resulting in a higher total number of cells (S5A and S5B Fig) and establishment of tdTomato-positive LPKO LCLs when trans-complemented with wild type EBNA-LP but not with the LRM mutant (Fig 4C and S5B and S5D Fig). These findings confirm that the conserved leucine-rich motifs are important for EBNA-LP activity in naïve B cells.

Trans-Complemented EBNA-LP Leucine-Rich Mutant is Expressed and Localizes Similar to Wild Type EBNA-LP in LCLs Derived from Adult Total B Cell Infection

We next sought to confirm that the EBNA-LP LRM mutant had wild type level expression. While the LRM mutant was unable to generate tdTomato positive LCLs from infected naïve B cells, LRM mutant transfected LPKO infections of total B cells yielded LCLs – presumably from transformation of memory B cells. Importantly, wild type and LRM mutant EBNA-LP were expressed at similar levels in these LCLs (Fig 5A). Furthermore, the LRM mutant was visible both in sub-nuclear puncta and diffuse within the nuclei of trans-complemented LPKO LCLs similar to wild

bioRxiv preprint doi: https://doi.org/10.1101/2024.01.07.574580; this version posted January 8, 2024. The copyright holder for this preprint (which was not certified by peer review) is the author/funder, who has granted bioRxiv a license to display the preprint in perpetuity. It is made available under aCC-BY 4.0 International license.

type EBNA-LP (Fig 5B). These results suggest mutation of the LRMs result in loss of an interaction between EBNA-LP and a cellular protein that is important for naïve B cell transformation, rather than loss of protein expression or misfolding.

Conserved Leucine-Rich Motifs in EBNA-LP are Required for Association with YY1

Given the role of leucine-rich motifs in coactivation by PGC family members, we used publicly available ChIP-Seq data from LCLs to identify cellular transcription factors whose binding sites on the genome had significant overlap with those of EBNA-LP. We found that YY1, a transcription factor co-activated by PGC proteins, shared many sites with EBNA-LP in agreement with previous work [18, 43, 44] (Fig 6A). The majority of overlapping sites occur at promoter regions (Fig 6B). To determine whether YY1 and EBNA-LP interact, we performed endogenous YY1 co-immunoprecipitation in EBV B95-8 strain derived LCLs for endogenous EBNA-LP. In three LCLs, YY1 pulled down EBNA-LP, further supporting complex formation between YY1 and EBNA-LP (Fig 6C).

As the interaction interface between EBNA-LP and YY1 is unknown, we investigated whether the leucine-rich motifs were indeed important. Using the trans-complemented LPKO LCLs derived from total B cells, reciprocal co-immunoprecipitations showed that wild type, but not LRM mutant EBNA-LP pulled down YY1 (Fig 6D), and conversely that YY1 co-immunoprecipitation pulled down wild type EBNA-LP, but not the LRM mutant protein (Fig 6E). Therefore, these LRM motifs in EBNA-LP that are required for transformation of naïve B cells are also required for interaction with the cellular transcription factor YY1, indicating a novel function for EBNA-LP in cellular transformation during EBV infection.

An essential role for YY1 in EBV infection and B cell transformation has not previously been described. Therefore, we used a Cas9 RNP-based knockout approach to assess the importance of YY1 in EBV-infected B cell outgrowth. The non-essential cell surface protein CD46 was used as a control and proxy for gene targeting as previously described by others [45]. We found that YY1 knockout in either total B cells (Fig 6F) or naïve B cells (Fig 6G) significantly reduced EBV-induced proliferation compared to the CD46 knockout control. These data complement our biochemical data and mutagenesis supporting a role for EBNA-LP and YY1 in EBV transformation of naïve B cells.

bioRxiv preprint doi: https://doi.org/10.1101/2024.01.07.574580; this version posted January 8, 2024. The copyright holder for this preprint (which was not certified by peer review) is the author/funder, who has granted bioRxiv a license to display the preprint in perpetuity. It is made available under aCC-BY 4.0 International license.

Discussion

EBV viral proteins aid in maintaining life-long, latently infected B cells by facilitating the proliferation and survival of infected cells. When the virus-host balance is disturbed, such as in the absence of a functional immune system, the characteristics of these viral proteins can contribute to oncogenesis as modeled by *in vitro* transformation of primary B cells by EBV. While EBNA-LP is essential for the transformation of naïve B cells by EBV, it has primarily been studied outside of the context of infection. As EBNA-LP is encoded in the viral genome across multiple repeat units of the major internal repeat, making mutations to the EBNA-LP coding sequence in the viral genome is particularly challenging and time consuming. Thus, we have developed a trans-complementation system by which the well-conserved regions of EBNA-LP could be assessed in the context of primary B cell infection.

Excitingly, we could reliably transfect resting primary B cells with an episomal construct that was maintained upon EBV infection and outgrowth into LCLs. This assay could therefore be used to screen a large number of EBNA-LP mutants in the context of EBV infection of primary B cells, beyond those we present here. This trans-complementation strategy presents a system by which it is possible to screen important functions of EBNA-LP so that the more precise but technically challenging and time-consuming approach of constructing mutant viruses can be more intelligently targeted. It also opens up the possibility of trans-complementing with proteins from other viruses that target the same biological processes, and can be adapted for trans-complementing EBV mutants more generally. Therefore, by pairing infection of knock-out viruses with trans-complementation of mutant viral proteins, this assay could be applied to identify key features of other viral proteins in EBV transformation of primary B cells.

Unexpectedly – given its importance for the perceived main function of EBNA-LP phosphorylation in EBNA2 co-activation – we found that EBNA-LP phosphorylation does not contribute detectably to the outgrowth of LCLs. As such, our work highlights both the limitations of studying viral proteins outside of the context of primary infection and suggests EBNA-LP has numerous roles in the survival and transformation of infected naïve B cells. Instead, we identified highly conserved leucine-rich motifs in both the W domain CR1 and Y domain CR4 that are required to rescue LPKO infected naïve B cells derived from adult peripheral blood and cord blood. While the presence of small numbers of antigen-experienced B cells – both conventional and double negative (IgD-/CD27-) memory B cells – in

bioRxiv preprint doi: https://doi.org/10.1101/2024.01.07.574580; this version posted January 8, 2024. The copyright holder for this preprint (which was not certified by peer review) is the author/funder, who has granted bioRxiv a license to display the preprint in perpetuity. It is made available under aCC-BY 4.0 International license.

our adult peripheral blood naïve B cell fractions led to outgrowth of some tdTomato negative LCLs, our results indicate that the leucine-rich motifs in EBNA-LP play an important role in EBV-mediated transformation.

We found the conserved leucine-rich motifs in EBNA-LP mediate interaction with YY1. YY1 is both a transcription factor and DNA looping factor that promotes interactions between enhancer and promoter regions [46]. YY1 is important in B cells as a transcriptional regulator of the germinal center reaction [47]. In the absence of YY1, naïve B cells are unable to differentiate into germinal center B cells or plasma cells [48-50]. The requirement for YY1 may in part be due to regulation of apoptosis, as YY1 knock out in pro-B cells and germinal center B cells causes cells to be more prone to apoptosis [48, 50]. YY1 deficient naïve B cells also display reduced proliferation upon stimulation compared to controls [48]. YY1 has also been implicated in transcriptional regulation of genes involved in oxidation phosphorylation in B cells [48, 49, 51], upregulation of which is required to avoid cellular arrest upon EBV infection [8]. As EBV-infected cells undergo B cell activation and differentiation in a manner that mimics the remodeling of antigen-experienced B cells through the germinal center [52, 53], YY1 may therefore be required for survival and effective cellular remodeling during EBV infection and transformation.

Furthermore, the unique importance for EBNA-LP in naïve and not memory B cell transformation upon EBV infection, suggests basal differences between naïve and memory B cells exist that require different strategies for viral transformation. Naïve B cells, for example, may require additional viral assistance in avoiding cell death compared to memory B cells, as naïve B cells express lower levels of antiapoptotic proteins and are more likely to undergo apoptosis in both the presence and absence of antigen stimulation than memory B cells [54]. Memory B cells also proliferate more rapidly upon antigen activation than naïve B cells [55, 56] as naïve B cells express elevated levels of negative cell cycle regulators [55]. Memory cells are also more predominantly in the cell cycle phase G_1 compared to naïve B cells [57], suggesting memory B cells are better primed to enter cell division while naïve B cells may have greater intrinsic barriers to EBV induction of proliferation. Further, naïve B cell activation by antigen increases both glycolysis and oxidative phosphorylation [58] and requires mitochondrial remodeling [59]. While little is known about the metabolic differences between resting naïve and memory B cells, memory T cells have increased mitochondrial mass compared to naïve T cells, and also have a greater capacity for both oxidative phosphorylation and glycolysis upon activation suggesting the transition from naïve to memory in immune cells alters metabolic capacity long term [60]. Therefore, EBNA-LP association with YY1 may be important in naïve B cells to overcome barriers to

bioRxiv preprint doi: https://doi.org/10.1101/2024.01.07.574580; this version posted January 8, 2024. The copyright holder for this preprint (which was not certified by peer review) is the author/funder, who has granted bioRxiv a license to display the preprint in perpetuity. It is made available under aCC-BY 4.0 International license.

transformation including apoptosis, initiation of proliferation, and cellular metabolism which may be innately more restrictive in naïve B cells than memory B cells. Additional functions of EBNA-LP including disruption of anti-viral PML nuclear bodies may also be important for elucidating the requirement for EBNA-LP in naïve B cell infection and outgrowth.

B cell activation and differentiation also requires a large degree of chromatin remodeling, which YY1, as a chromatin looping factor, may contribute to. During the transition from naïve B cells to germinal center B cells, roughly 95% of chromatin compartments are remodeled, primarily to a more active chromatin state, followed by 73% of remodeled regions returning to their original states in memory B cells [61]. EBV infection largely mimics this chromatin remodeling process [62], however, whether differences in naïve and memory B cell chromatin architecture includes YY1 motif accessibility or YY1-regulated DNA loops remains to be studied, but could provide insight as to further differences in naïve B cell dependence on EBNA-LP and YY1 association.

As a mechanism for cellular gene regulation, YY1 has also been implicated in the formation of “EBV super-enhancers” on host chromatin, which are defined as regions of accessible chromatin where multiple EBNAs and cellular transcription factors associate leading to increased expression of target genes [63]. “EBV super-enhancers” target genes important in infected cell survival and proliferation including Myc [63]. Therefore, EBNA-LP association with YY1 for genome rearrangement may in fact be a mechanism by which EBNA-LP stabilizes induction of EBNA2 associated genes, including both important cellular genes and viral genes. YY1 is able to alter the structure and epigenetic marks of numerous DNA virus genomes resulting in both activation and repression of viral genes [64]. These viruses include herpesviruses such as Human Cytomegalovirus and Kaposi’s Sarcoma-Associated Herpesvirus, small DNA tumor viruses including Human Papilloma Virus, and many others [64-68]. In the EBV genome, YY1 binds and represses the promoters of the immediate early genes BZLF1 and BRLF1, preventing induction of the productive replication cycle [69-71]. There is also a YY1 binding site upstream of the immediate-early latency promoter Wp [72]. This region including the YY1 binding site is important for transcription from both the Cp and initial Wp, and deletion hinders transformation of infected cells [73]. Therefore, YY1 binding to the viral genome may contribute to inducing adequate expression of viral latency proteins through regulation of viral Wp and Cp promoter usage during early infection and transformation. Whether YY1 occurrence at these cellular and viral genomic sites is EBNA-LP dependent requires further investigation.

bioRxiv preprint doi: https://doi.org/10.1101/2024.01.07.574580; this version posted January 8, 2024. The copyright holder for this preprint (which was not certified by peer review) is the author/funder, who has granted bioRxiv a license to display the preprint in perpetuity. It is made available under aCC-BY 4.0 International license.

Overall, this study identifies previously uncharacterized, yet highly conserved, motifs within EBNA-LP that are important for transformation of EBV-infected naïve B cells. This work suggests EBNA-LP encodes leucine-rich motifs to engage the important cellular transcription factor YY1 for EBV-induced cellular transformation.

Materials and Methods

Virus Preparation

LPKO virus refers to LPKO^{w} from Szymula et al. [32] encoding stop codons in every internal W repeat. Wild Type EBV (WT) refers to the WT^{w} from Szymula et al. [32] that has a stop codon repaired in the parental B95-8 genome, and encodes a total of 6 W repeats. Viruses were prepared from 293-EBV producer lines and Raji Green Unit titer was obtained as previously described, using flow cytometry to count green cells [32, 74]. B95-8 strain of EBV was produced from the B95-8 Z-HT cell line as previously described [75].

Cell Culture and Cell Isolation

Adult buffy coats were obtained from the Gulf Coast Regional Blood Center (Pro00006262) and cord blood was obtained from the Carolinas Cord Blood Bank (Pro00061264). Peripheral blood mononuclear cells were isolated using Histopaque-1077 (Sigma, H8889) and SepMate PBMC Isolation tubes. Naïve B cells were then isolated from adult blood using the EasySep Human Memory B Cell Isolation kit (STEMCELL Technologies #17864) to first remove CD27 positive memory cells, followed by negative isolation of B cells. To obtain total B cells, the Easy Human Pan-B Cell Enrichment kit (STEMCELL Technologies #19554) was used. Purity of isolated cells was assessed by flow cytometry with antibodies to CD19, IgD, and CD27 (Table 1). Primary cells were maintained in Roswell Park Memorial Institute (RPMI) medium 1640 supplemented with 20% heat-inactivated fetal bovine serum (FBS) (Corning). LCLs and BJAB cell lines were maintained in RPMI supplemented with 10% FBS and 2 mM L-glutamine, penicillin/streptomycin. 293T cells were maintained in Dulbecco's Modified Eagle Medium (DMEM) with 10% FBS.

DNA Constructs

EBNA-LP cDNA was synthesized (GENEWIZ) to encode wild type (B95-8) EBNA-LP or mutants containing four copies of the W repeat domain (S1 Table). Codon usage of this repeat was modified such that the amino acid

bioRxiv preprint doi: https://doi.org/10.1101/2024.01.07.574580; this version posted January 8, 2024. The copyright holder for this preprint (which was not certified by peer review) is the author/funder, who has granted bioRxiv a license to display the preprint in perpetuity. It is made available under aCC-BY 4.0 International license.

sequence in each W domain was identical, but the DNA sequence in each W domain was unique in order to avoid recombination of repeated W domains and facilitate downstream cloning. S3A and S3E EBNA-LP genes were synthesized with the S34, S36, and S63 in each W domain modified to alanine or glutamic acid respectively. For the LRM mutant, EBNA-LP cDNA was first synthesized such that L25, L28, and L29 in each W domain were modified to alanine. QuikChange XL Site-Directed Mutagenesis (Agilent, 200517) was then used to modify L13, L17, and L18 in the Y domain to alanine.

Table 1. Reagents and materials used in methods.

Name	Company	Catalog. No.	Concentration
JF186 Antibody (EBNA-LP)	Purified in house to 1 mg/mL	NA	Western blot 1:500, Immunofluorescence 1:100
YY1 Monoclonal Antibody	Proteintech	66281-1-Ig	1:500, IP
YY1 (D5D9Z)	Cell Signaling Technology	46395S	1:1000, western blot
YY1 antibody (pAb)	Active Motif	61779	1:1000, western blot
Anti-Mouse IgG-Peroxidase	Sigma-Aldrich	A9044-2ML	1:5000, western blot
Anti-Rabbit IgG-Peroxidase	Sigma-Aldrich	A0545-1ML	1:3000, western blot
VeriBlot	Abcam	ab131366	1:500, western blot
Alexa Fluor 488 goat anti-mouse IgG (H+L)	ThermoFisher Scientific	A11001	1:250, immunofluorescence
Normal Mouse IgG1	Santa Cruz	sc-3877	5 ng per IP
Normal Mouse IgG2a	Santa Cruz	sc-3878	5 ng per IP
Anti-FLAG M2 Antibody	Sigma-Aldrich	F1804	1:100 , IP
CD46 PE	BioLegend	352402	1:100, Flow Cytometry
IgD PE/Cy7	BioLegend	348217	1:100, Flow Cytometry
CD27 AlexaFluor 488	BioLegend	393204	1:100, Flow Cytometry
CD19 APC	BioLegend	302212	1:100, Flow Cytometry
cOmplete, mini, EDTA-free Protease Inhibitor Cocktails	Roche	4693159001	1x protein lysates, 2x IP
PhosSTOP	Roche	4906837001	1x
CD46 Guide #1	SYNTHEGO	GAGAAACAUGUCCAUAUAUA	
CD46 Guide #2	SYNTHEGO	AACUCGUAAGUCCCAUUUGC	
CD46 Guide #3	SYNTHEGO	UUGCUCCUUAGAGGAAAUAA	
YY1 Guide #1	SYNTHEGO	CUGGUCACCGUGGCGGCGGC	
YY1 Guide #2	SYNTHEGO	GGAGGCGGCCGCGUCAAGAA	
YY1 Guide #3	SYNTHEGO	CGACCCGGGCAACAAGAAGU	

bioRxiv preprint doi: https://doi.org/10.1101/2024.01.07.574580; this version posted January 8, 2024. The copyright holder for this preprint (which was not certified by peer review) is the author/funder, who has granted bioRxiv a license to display the preprint in perpetuity. It is made available under aCC-BY 4.0 International license.

EBNA-LP constructs were first cloned into pSG5-FLAG-Gateway (a gift from Eric Johannsen) for expression in 293T cells by amplifying with primers encoding attB1/attB2 recombination sites and performing recombination by gateway cloning (ThermoFisher 11789020, and 11791020). For trans-complementation assays, FLAG-tdTomato-P2A was cloned into pCEP4 vector by restriction digest cloning. FLAG-EBNA-LP constructs were then cloned into this vector using XhoI and BamHI restriction sites immediately following the P2A cleavage site (**S1 Fig**). Following P2A cleavage, EBNA-LP protein includes a proline (site of cleavage), FLAG epitope, linker including the attB1 recombination site from gateway cloning, and full-length EBNA-LP (**S1 Fig**).

Trans-complementation Assays

Purified adult naïve or cord blood B cells were resuspended in Belzer UW Cold Storage Solution (BridgetoLife) at 480,000 cells/7 μL and combined with 1.2 μg of DNA in 5 μL Buffer T (Neon Transfection Kit) for excess volume to avoid air bubbles. As 10 μL tips were used for transfect, approximately 400,000 cells total were transfected per replicate. DNA was prepared by maxi prep (ZymoPURE, D4203), eluting DNA in Buffer T (Neon Transfection Kit). Cells were transfected using the Thermo Fisher Neon Transfection System at 2150 V, 20 ms, 1 pulse, 10 μL tips and resuspended in 200 μL RPMI with 20% FBS. One hour after transfection, cells were infected with LPKO or WT virus at 0.2 Raji Green Units per cell for 1 hour at 37° C, a ratio we previously determined by EBNA2 immunofluorescence to infect almost all B cells and an optimal ratio for outgrowth, similar to previous reports [9]. Every seven days, cell outgrowth was quantified by flow cytometry. Media was added during outgrowth upon increased cell density.

Flow Cytometry

Flow cytometry was used to assess purity of isolated primary cells and to quantify outgrowth of trans-complemented naïve B cells. For sample preparation following isolation, cells were washed once in FACS Buffer (PBS with 2% FBS), stained with indicated antibodies (Table 1) for 15 minutes in the dark at room temperature, then rinsed again with FACS buffer. For samples in the trans-complement assays, samples were prepared and collected in a 96-well V-bottom plate. First, samples were evenly resuspended, and a known volume of each sample was moved to the plate. Samples were then washed once in FACS buffer and resuspended in 100 uL of FACS buffer prior to collection. Samples were collected using the BD FACSCanto-II with a high throughput sampler to collect precise sample volumes. Analysis was performed using FlowJo software (FlowJo, LLC).

bioRxiv preprint doi: https://doi.org/10.1101/2024.01.07.574580; this version posted January 8, 2024. The copyright holder for this preprint (which was not certified by peer review) is the author/funder, who has granted bioRxiv a license to display the preprint in perpetuity. It is made available under aCC-BY 4.0 International license.

Amino Acid Sequence Alignment

Alignment was performed with Geneious Prime 2023.1.2 (https://www.geneious.com) multiple sequence alignment. The LCV Baboon, Gorilla, and Chimpanzee strains were previously published [24]. The remaining sequences were obtained from NCBI (NC_007605.1, NC_006146.1, NC_009334.1). Number was specified from internal W domain amino acid sequence for consistency, rather than number from the start codon.

293T FLAG Immunoprecipitation

293T cells were transfected with 20 μg DNA followed by media change the next day. Three days post-transfection, cells were washed twice with cold PBS followed by addition of lysis buffer (150 mM NaCl, 0.5% Sodium Deoxycholate, 1% NP-40, 50 mM Tris pH 8, 10% glycerol, 2x protease inhibitor, 1x phosphatase inhibitor (Table 1**)**. Cells were scraped and lysates were shaken for 30 minutes at 600 rpm at 4°C followed by centrifugation at maximum speed for 10 minutes. Lysates were pre-cleared with Dynabeads Protein G (ThermoFisher, 10004D) conjugated to Normal Mouse IgG (Table 1**)**. Lysates were quantified by Bradford assay (Bio-Rad, 5000006) and 1 mg of protein was used per condition. Lysates were rotated with antibody overnight with rotation. Dynabeads were added and incubated for 3 hours at 4°C while rotating. After incubation, beads were washed four times in wash buffer (150 mM NaCl, 0.5% NP-40, 50 mM Tris pH 8, 10% glycerol, 1x protease inhibitor, 1x phosphatase inhibitor) and eluted in 1x LDS Sample Buffer (ThermoFisher, NP0007) by boiling 10 minutes at 55°C.

Co-Immunoprecipitations in LCLs

40-50 million cells were pelleted, washed once in PBS, and resuspended in cold lysis buffer (150 mM NaCl, 50 mM Tris pH 7.6, 1% NP-40, 2 mM EDTA, sodium molybdate, 2x protease inhibitor, 1x phosphatase inhibitor). Lysates were prepared as described above for FLAG Immunoprecipitations. Input was stored with 1x LDS Sample Buffer after pre-clear. Beads were washed four times with fresh, ice-cold lysis buffer (YY1 co-immunoprecipitations in B95-8 derived LCLs) or lysis buffer with 0.5% NP-40 (FLAG and YY1 co-immunoprecipitations in LPKO trans-complemented LCLs). Samples were eluted in 1X LDS Sample Buffer by boiling at 37°C for 10 minutes.

Western Blotting

bioRxiv preprint doi: https://doi.org/10.1101/2024.01.07.574580; this version posted January 8, 2024. The copyright holder for this preprint (which was not certified by peer review) is the author/funder, who has granted bioRxiv a license to display the preprint in perpetuity. It is made available under aCC-BY 4.0 International license.

Cells were washed one time with PBS before pelleting. Pellets were resuspended in 1x RIPA buffer with protease and phosphatase inhibitors added. After shaking samples at 4°C at 600 rpm, samples were centrifuged for 10 minutes at 14,000xg. The lysates were then quantified using Bradford assay and diluted to 1x LDS. Samples were loaded on a 4-12% Bis-Tris gel (ThermoFisher, NP0321BOX) and run in MOPS Running Buffer (ThermoFisher, NP0001) followed by transfer to PVDF membranes using a TransBlot Turbo Transfer System at 25 V, 1.3 A, for 12 min (Bio-Rad). Total protein was quantified using total protein stain (LI-COR, 926-11011) and blocked in 5% milk in 1x TBST. Blot was incubated overnight with primary antibody in 1x TBST with 5% BSA at 4°C. Blots were then washed in 1x TBST, incubated in secondary antibody for 1 hour at room temperature in 5% milk, and washed three times for 10 minutes. Blots were incubated with HRP substrate and imaged on the LI-COR Odyssey XF Imager.

Immunofluorescence

Immunofluorescence was performed as described previously [8]. Slides were mounted in VECTASHIELD HardSet Antifade Mounting medium with DAPI (H-1500-10). Slides were imaged using the Olympus IX81 microscope using a 60X oil objective.

ChIP-Seq Analysis

Analysis of YY1 and EBNA-LP ChIP-Seq data was performed using HOMER [76]. The functions makeTagDirectory and findPeaks were used to call YY1 peaks. EBNA-LP called peaks were obtained as previously described [18]. The function mergePeaks with a distance of 200 base pairs was used to identify overlapping and uniquely bound sites between YY1 and EBNA-LP. The function annotatePeaks.pl was then used to assign overlapping peaks to genomic regions. YY1 ChIP-Seq in GM12878 data was obtained from ENCODE (Experiment ENCSR000BNP).

Cas9-RNP Transfection

TrueCut Cas9 protein-v2 (ThermoFisher, A36499), 10 pmol per target, was incubated with 30 pmol sgRNA (Gene Knockout Kit v2, Synthego) per target (Table 1). Isolated naïve and total B cells were washed in PBS and resuspended in Buffer T (Neon Transfection System). 350,000 cells were transfected with Cas9/RNP complexes and infected with B95-8 virus as described above. Outgrowth was assessed by flow cytometry upon staining cells with anti-CD46 (Table 1).

bioRxiv preprint doi: https://doi.org/10.1101/2024.01.07.574580; this version posted January 8, 2024. The copyright holder for this preprint (which was not certified by peer review) is the author/funder, who has granted bioRxiv a license to display the preprint in perpetuity. It is made available under aCC-BY 4.0 International license.

Mass Spectrometry

See S1 Text for extended methods.

Acknowledgements

This work was funded by NIH grant R01CA140337 (to M.A.L.), T32CA009111 (M.A.L.), and F31DE031509 (to J.M.C.). We acknowledge Ashley P. Barry and Marc Leazer for generation of reagents. We thank the Duke University School of Medicine for the use of the Proteomics and Metabolomics Core Facility, which provided mass spectrometry services, and Erik Soderblom for assistance in interpreting the mass spectrometry data. We also acknowledge the ENCODE Consortium and the lab of Richard Myers for generating the YY1 ChIP-Seq data. Research reported in this publication was supported in part by the Office of The Director of the National Institutes of Health under Award Number S10OD024999. The content is solely the responsibility of the authors and does not necessarily represent the official views of the National Institutes of Health.

References

1. Babcock GJ, Decker LL, Volk M, Thorley-Lawson DA. EBV persistence in memory B cells in vivo. Immunity. 1998;9(3):395-404.
2. Shannon-Lowe C, Rickinson AB, Bell AI. Epstein-Barr virus-associated lymphomas. Philos Trans R Soc Lond B Biol Sci. 2017;372(1732).
3. Szekely L, Pokrovskaja K, Jiang WQ, Selivanova G, Lowbeer M, Ringertz N, et al. Resting B-cells, EBV-infected B-blasts and established lymphoblastoid cell lines differ in their Rb, p53 and EBNA-5 expression patterns. Oncogene. 1995;10(9):1869-74.
4. Sinclair AJ, Palmero I, Peters G, Farrell PJ. EBNA-2 and EBNA-LP cooperate to cause G0 to G1 transition during immortalization of resting human B lymphocytes by Epstein-Barr virus. EMBO J. 1994;13(14):3321-8.
5. Alfieri C, Birkenbach M, Kieff E. Early events in Epstein-Barr virus infection of human B lymphocytes. Virology. 1991;181(2):595-608.
6. Price AM, Tourigny JP, Forte E, Salinas RE, Dave SS, Luftig MA. Analysis of Epstein-Barr virus-regulated host gene expression changes through primary B-cell outgrowth reveals delayed kinetics of latent membrane protein 1-mediated NF-kappaB activation. J Virol. 2012;86(20):11096-106.
7. Nikitin PA, Yan CM, Forte E, Bocedi A, Tourigny JP, White RE, et al. An ATM/Chk2-mediated DNA damage-responsive signaling pathway suppresses Epstein-Barr virus transformation of primary human B cells. Cell Host Microbe. 2010;8(6):510-22.
8. McFadden K, Hafez AY, Kishton R, Messinger JE, Nikitin PA, Rathmell JC, Luftig MA. Metabolic stress is a barrier to Epstein-Barr virus-mediated B-cell immortalization. Proc Natl Acad Sci U S A. 2016;113(6):E782-90.

bioRxiv preprint doi: https://doi.org/10.1101/2024.01.07.574580; this version posted January 8, 2024. The copyright holder for this preprint (which was not certified by peer review) is the author/funder, who has granted bioRxiv a license to display the preprint in perpetuity. It is made available under aCC-BY 4.0 International license.

9. Pich D, Mrozek-Gorska P, Bouvet M, Sugimoto A, Akidil E, Grundhoff A, et al. First Days in the Life of Naive Human B Lymphocytes Infected with Epstein-Barr Virus. mBio. 2019;10(5).
10. Kaiser C, Laux G, Eick D, Jochner N, Bornkamm GW, Kempkes B. The proto-oncogene c-myc is a direct target gene of Epstein-Barr virus nuclear antigen 2. J Virol. 1999;73(5):4481-4.
11. Zimber-Strobl U, Strobl LJ, Meitinger C, Hinrichs R, Sakai T, Furukawa T, et al. Epstein-Barr virus nuclear antigen 2 exerts its transactivating function through interaction with recombination signal binding protein RBP-J kappa, the homologue of Drosophila Suppressor of Hairless. EMBO J. 1994;13(20):4973-82.
12. Glaser LV, Rieger S, Thumann S, Beer S, Kuklik-Roos C, Martin DE, et al. EBF1 binds to EBNA2 and promotes the assembly of EBNA2 chromatin complexes in B cells. PLoS Pathog. 2017;13(10):e1006664.
13. Harada S, Kieff E. Epstein-Barr virus nuclear protein LP stimulates EBNA-2 acidic domain-mediated transcriptional activation. J Virol. 1997;71(9):6611-8.
14. Nitsche F, Bell A, Rickinson A. Epstein-Barr virus leader protein enhances EBNA-2-mediated transactivation of latent membrane protein 1 expression: a role for the W1W2 repeat domain. J Virol. 1997;71(9):6619-28.
15. Portal D, Zhao B, Calderwood MA, Sommermann T, Johannsen E, Kieff E. EBV nuclear antigen EBNALP dismisses transcription repressors NCoR and RBPJ from enhancers and EBNA2 increases NCoR-deficient RBPJ DNA binding. Proc Natl Acad Sci U S A. 2011;108(19):7808-13.
16. Portal D, Rosendorff A, Kieff E. Epstein-Barr nuclear antigen leader protein coactivates transcription through interaction with histone deacetylase 4. Proc Natl Acad Sci U S A. 2006;103(51):19278-83.
17. Han I, Xue Y, Harada S, Orstavik S, Skalhegg B, Kieff E. Protein kinase A associates with HA95 and affects transcriptional coactivation by Epstein-Barr virus nuclear proteins. Mol Cell Biol. 2002;22(7):2136-46.
18. Portal D, Zhou H, Zhao B, Kharchenko PV, Lowry E, Wong L, et al. Epstein-Barr virus nuclear antigen leader protein localizes to promoters and enhancers with cell transcription factors and EBNA2. Proc Natl Acad Sci U S A. 2013;110(46):18537-42.
19. Szekely L, Pokrovskaja K, Jiang WQ, de The H, Ringertz N, Klein G. The Epstein-Barr virus-encoded nuclear antigen EBNA-5 accumulates in PML-containing bodies. J Virol. 1996;70(4):2562-8.
20. Ling PD, Peng RS, Nakajima A, Yu JH, Tan J, Moses SM, et al. Mediation of Epstein-Barr virus EBNA-LP transcriptional coactivation by Sp100. EMBO J. 2005;24(20):3565-75.
21. Tierney RJ, Kao KY, Nagra JK, Rickinson AB. Epstein-Barr virus BamHI W repeat number limits EBNA2/EBNA-LP coexpression in newly infected B cells and the efficiency of B-cell transformation: a rationale for the multiple W repeats in wild-type virus strains. J Virol. 2011;85(23):12362-75.
22. Peng R, Gordadze AV, Fuentes Panana EM, Wang F, Zong J, Hayward GS, et al. Sequence and functional analysis of EBNA-LP and EBNA2 proteins from nonhuman primate lymphocryptoviruses. J Virol. 2000;74(1):379-89.
23. Peng R, Tan J, Ling PD. Conserved regions in the Epstein-Barr virus leader protein define distinct domains required for nuclear localization and transcriptional cooperation with EBNA2. J Virol. 2000;74(21):9953-63.
24. McCann EM, Kelly GL, Rickinson AB, Bell AI. Genetic analysis of the Epstein-Barr virus-coded leader protein EBNA-LP as a co-activator of EBNA2 function. J Gen Virol. 2001;82(Pt 12):3067-79.
25. Petti L, Sample C, Kieff E. Subnuclear localization and phosphorylation of Epstein-Barr virus latent infection nuclear proteins. Virology. 1990;176(2):563-74.
26. Sauter M, Boos H, Hirsch F, Mueller-Lantzsch N. Characterization of a latent protein encoded by the large internal repeats and the BamHI Y fragment of the Epstein-Barr virus (EBV) genome. Virology. 1988;166(2):586-90.

bioRxiv preprint doi: https://doi.org/10.1101/2024.01.07.574580; this version posted January 8, 2024. The copyright holder for this preprint (which was not certified by peer review) is the author/funder, who has granted bioRxiv a license to display the preprint in perpetuity. It is made available under aCC-BY 4.0 International license.

27. Kitay MK, Rowe DT. Cell cycle stage-specific phosphorylation of the Epstein-Barr virus immortalization protein EBNA-LP. J Virol. 1996;70(11):7885-93.
28. Han I, Harada S, Weaver D, Xue Y, Lane W, Orstavik S, et al. EBNA-LP associates with cellular proteins including DNA-PK and HA95. J Virol. 2001;75(5):2475-81.
29. Yokoyama A, Tanaka M, Matsuda G, Kato K, Kanamori M, Kawasaki H, et al. Identification of major phosphorylation sites of Epstein-Barr virus nuclear antigen leader protein (EBNA-LP): ability of EBNA-LP to induce latent membrane protein 1 cooperatively with EBNA-2 is regulated by phosphorylation. J Virol. 2001;75(11):5119-28.
30. Kato K, Yokoyama A, Tohya Y, Akashi H, Nishiyama Y, Kawaguchi Y. Identification of protein kinases responsible for phosphorylation of Epstein-Barr virus nuclear antigen leader protein at serine-35, which regulates its coactivator function. J Gen Virol. 2003;84(Pt 12):3381-92.
31. Wang C, Zhou H, Xue Y, Liang J, Narita Y, Gerdt C, et al. Epstein-Barr Virus Nuclear Antigen Leader Protein Coactivates EP300. J Virol. 2018;92(9).
32. Szymula A, Palermo RD, Bayoumy A, Groves IJ, Ba Abdullah M, Holder B, White RE. Epstein-Barr virus nuclear antigen EBNA-LP is essential for transforming naive B cells, and facilitates recruitment of transcription factors to the viral genome. PLoS Pathog. 2018;14(2):e1006890.
33. Hammerschmidt W, Sugden B. Genetic analysis of immortalizing functions of Epstein-Barr virus in human B lymphocytes. Nature. 1989;340(6232):393-7.
34. Mannick JB, Cohen JI, Birkenbach M, Marchini A, Kieff E. The Epstein-Barr virus nuclear protein encoded by the leader of the EBNA RNAs is important in B-lymphocyte transformation. J Virol. 1991;65(12):6826-37.
35. Igarashi M, Kawaguchi Y, Hirai K, Mizuno F. Physical interaction of Epstein-Barr virus (EBV) nuclear antigen leader protein (EBNA-LP) with human oestrogen-related receptor 1 (hERR1): hERR1 interacts with a conserved domain of EBNA-LP that is critical for EBV-induced B-cell immortalization. J Gen Virol. 2003;84(Pt 2):319-27.
36. Huss JM, Kopp RP, Kelly DP. Peroxisome proliferator-activated receptor coactivator-1alpha (PGC-1alpha) coactivates the cardiac-enriched nuclear receptors estrogen-related receptor-alpha and -gamma. Identification of novel leucine-rich interaction motif within PGC-1alpha. J Biol Chem. 2002;277(43):40265-74.
37. Heery DM, Kalkhoven E, Hoare S, Parker MG. A signature motif in transcriptional co-activators mediates binding to nuclear receptors. Nature. 1997;387(6634):733-6.
38. Torchia J, Rose DW, Inostroza J, Kamei Y, Westin S, Glass CK, Rosenfeld MG. The transcriptional co-activator p/CIP binds CBP and mediates nuclear-receptor function. Nature. 1997;387(6634):677-84.
39. Wei C, Anolik J, Cappione A, Zheng B, Pugh-Bernard A, Brooks J, et al. A new population of cells lacking expression of CD27 represents a notable component of the B cell memory compartment in systemic lupus erythematosus. J Immunol. 2007;178(10):6624-33.
40. Benore-Parsons M, Seidah NG, Wennogle LP. Substrate phosphorylation can inhibit proteolysis by trypsin-like enzymes. Arch Biochem Biophys. 1989;272(2):274-80.
41. Winter D, Kugelstadt D, Seidler J, Kappes B, Lehmann WD. Protein phosphorylation influences proteolytic cleavage and kinase substrate properties exemplified by analysis of in vitro phosphorylated Plasmodium falciparum glideosome-associated protein 45 by nano-ultra performance liquid chromatography-tandem mass spectrometry. Anal Biochem. 2009;393(1):41-7.
42. Budeus B, Kibler A, Brauser M, Homp E, Bronischewski K, Ross JA, et al. Human Cord Blood B Cells Differ from the Adult Counterpart by Conserved Ig Repertoires and Accelerated Response Dynamics. J Immunol. 2021;206(12):2839-51.
43. Luo Y, Hitz BC, Gabdank I, Hilton JA, Kagda MS, Lam B, et al. New developments on the Encyclopedia of DNA Elements (ENCODE) data portal. Nucleic Acids Res. 2020;48(D1):D882-D9.

bioRxiv preprint doi: https://doi.org/10.1101/2024.01.07.574580; this version posted January 8, 2024. The copyright holder for this preprint (which was not certified by peer review) is the author/funder, who has granted bioRxiv a license to display the preprint in perpetuity. It is made available under aCC-BY 4.0 International license.

44. Cunningham JT, Rodgers JT, Arlow DH, Vazquez F, Mootha VK, Puigserver P. mTOR controls mitochondrial oxidative function through a YY1-PGC-1alpha transcriptional complex. Nature. 2007;450(7170):736-40.
45. Akidil E, Albanese M, Buschle A, Ruhle A, Pich D, Keppler OT, Hammerschmidt W. Highly efficient CRISPR-Cas9-mediated gene knockout in primary human B cells for functional genetic studies of Epstein-Barr virus infection. PLoS Pathog. 2021;17(4):e1009117.
46. Weintraub AS, Li CH, Zamudio AV, Sigova AA, Hannett NM, Day DS, et al. YY1 Is a Structural Regulator of Enhancer-Promoter Loops. Cell. 2017;171(7):1573-88 e28.
47. Green MR, Monti S, Dalla-Favera R, Pasqualucci L, Walsh NC, Schmidt-Supprian M, et al. Signatures of murine B-cell development implicate Yy1 as a regulator of the germinal center-specific program. Proc Natl Acad Sci U S A. 2011;108(7):2873-8.
48. Kleiman E, Jia H, Loguercio S, Su AI, Feeney AJ. YY1 plays an essential role at all stages of B-cell differentiation. Proc Natl Acad Sci U S A. 2016;113(27):E3911-20.
49. Banerjee A, Sindhava V, Vuyyuru R, Jha V, Hodewadekar S, Manser T, Atchison ML. YY1 Is Required for Germinal Center B Cell Development. PLoS One. 2016;11(5):e0155311.
50. Trabucco SE, Gerstein RM, Zhang H. YY1 Regulates the Germinal Center Reaction by Inhibiting Apoptosis. J Immunol. 2016;197(5):1699-707.
51. Nandi S, Liang G, Sindhava V, Angireddy R, Basu A, Banerjee S, et al. YY1 control of mitochondrial-related genes does not account for regulation of immunoglobulin class switch recombination in mice. Eur J Immunol. 2020;50(6):822-38.
52. SoRelle ED, Dai J, Reinoso-Vizcaino NM, Barry AP, Chan C, Luftig MA. Time-resolved transcriptomes reveal diverse B cell fate trajectories in the early response to Epstein-Barr virus infection. Cell Rep. 2022;40(9):111286.
53. Roughan JE, Thorley-Lawson DA. The intersection of Epstein-Barr virus with the germinal center. J Virol. 2009;83(8):3968-76.
54. Good KL, Avery DT, Tangye SG. Resting human memory B cells are intrinsically programmed for enhanced survival and responsiveness to diverse stimuli compared to naive B cells. J Immunol. 2009;182(2):890-901.
55. Good KL, Tangye SG. Decreased expression of Kruppel-like factors in memory B cells induces the rapid response typical of secondary antibody responses. Proc Natl Acad Sci U S A. 2007;104(33):13420-5.
56. Tangye SG, Avery DT, Deenick EK, Hodgkin PD. Intrinsic differences in the proliferation of naive and memory human B cells as a mechanism for enhanced secondary immune responses. J Immunol. 2003;170(2):686-94.
57. Moens L, Kane A, Tangye SG. Naive and memory B cells exhibit distinct biochemical responses following BCR engagement. Immunol Cell Biol. 2016;94(8):774-86.
58. Price MJ, Patterson DG, Scharer CD, Boss JM. Progressive Upregulation of Oxidative Metabolism Facilitates Plasmablast Differentiation to a T-Independent Antigen. Cell Rep. 2018;23(11):3152-9.
59. Waters LR, Ahsan FM, Wolf DM, Shirihai O, Teitell MA. Initial B Cell Activation Induces Metabolic Reprogramming and Mitochondrial Remodeling. iScience. 2018;5:99-109.
60. van der Windt GJ, O'Sullivan D, Everts B, Huang SC, Buck MD, Curtis JD, et al. CD8 memory T cells have a bioenergetic advantage that underlies their rapid recall ability. Proc Natl Acad Sci U S A. 2013;110(35):14336-41.
61. Vilarrasa-Blasi R, Soler-Vila P, Verdaguer-Dot N, Russinol N, Di Stefano M, Chapaprieta V, et al. Dynamics of genome architecture and chromatin function during human B cell differentiation and neoplastic transformation. Nat Commun. 2021;12(1):651.

bioRxiv preprint doi: https://doi.org/10.1101/2024.01.07.574580; this version posted January 8, 2024. The copyright holder for this preprint (which was not certified by peer review) is the author/funder, who has granted bioRxiv a license to display the preprint in perpetuity. It is made available under aCC-BY 4.0 International license.

62. SoRelle ED, Reinoso-Vizcaino NM, Dai J, Barry AP, Chan C, Luftig MA. Epstein-Barr virus evades restrictive host chromatin closure by subverting B cell activation and germinal center regulatory loci. Cell Rep. 2023;42(8):112958.
63. Zhou H, Schmidt SC, Jiang S, Willox B, Bernhardt K, Liang J, et al. Epstein-Barr virus oncoprotein super-enhancers control B cell growth. Cell Host Microbe. 2015;17(2):205-16.
64. Pentland I, Campos-Leon K, Cotic M, Davies KJ, Wood CD, Groves IJ, et al. Disruption of CTCF-YY1-dependent looping of the human papillomavirus genome activates differentiation-induced viral oncogene transcription. PLoS Biol. 2018;16(10):e2005752.
65. Chang PJ, Chen LW, Shih YC, Tsai PH, Liu AC, Hung CH, et al. Role of the cellular transcription factor YY1 in the latent-lytic switch of Kaposi's sarcoma-associated herpesvirus. Virology. 2011;413(2):194-204.
66. Poole E, Carlan da Silva MC, Huang C, Perera M, Jackson S, Groves IJ, et al. A BMPR2/YY1 Signaling Axis Is Required for Human Cytomegalovirus Latency in Undifferentiated Myeloid Cells. mBio. 2021;12(3):e0022721.
67. Liu R, Baillie J, Sissons JG, Sinclair JH. The transcription factor YY1 binds to negative regulatory elements in the human cytomegalovirus major immediate early enhancer/promoter and mediates repression in non-permissive cells. Nucleic Acids Res. 1994;22(13):2453-9.
68. Warowicka A, Broniarczyk J, Weglewska M, Kwasniewski W, Gozdzicka-Jozefiak A. Dual Role of YY1 in HPV Life Cycle and Cervical Cancer Development. Int J Mol Sci. 2022;23(7).
69. Montalvo EA, Cottam M, Hill S, Wang YJ. YY1 binds to and regulates cis-acting negative elements in the Epstein-Barr virus BZLF1 promoter. J Virol. 1995;69(7):4158-65.
70. Zalani S, Coppage A, Holley-Guthrie E, Kenney S. The cellular YY1 transcription factor binds a cis-acting, negatively regulating element in the Epstein-Barr virus BRLF1 promoter. J Virol. 1997;71(4):3268-74.
71. Chang LK, Liu ST. Activation of the BRLF1 promoter and lytic cycle of Epstein-Barr virus by histone acetylation. Nucleic Acids Res. 2000;28(20):3918-25.
72. Bell A, Skinner J, Kirby H, Rickinson A. Characterisation of regulatory sequences at the Epstein-Barr virus BamHI W promoter. Virology. 1998;252(1):149-61.
73. Yoo LI, Woloszynek J, Templeton S, Speck SH. Deletion of Epstein-Barr virus regulatory sequences upstream of the EBNA gene promoter Wp1 is unfavorable for B-Cell immortalization. J Virol. 2002;76(22):11763-9.
74. Sashihara J, Burbelo PD, Savoldo B, Pierson TC, Cohen JI. Human antibody titers to Epstein-Barr Virus (EBV) gp350 correlate with neutralization of infectivity better than antibody titers to EBV gp42 using a rapid flow cytometry-based EBV neutralization assay. Virology. 2009;391(2):249-56.
75. Johannsen E, Luftig M, Chase MR, Weicksel S, Cahir-McFarland E, Illanes D, et al. Proteins of purified Epstein-Barr virus. Proc Natl Acad Sci U S A. 2004;101(46):16286-91.
76. Heinz S, Benner C, Spann N, Bertolino E, Lin YC, Laslo P, et al. Simple combinations of lineage-determining transcription factors prime cis-regulatory elements required for macrophage and B cell identities. Mol Cell. 2010;38(4):576-89.

Figures

Fig 1. Trans-complementation rescues LPKO virus infected naïve B cells.
A. Schematic of experimental design. **B.** Outgrowth of tdTomato positive cells over time (n=3). WT infected cells are indicated with dashed lines, while LPKO infected cells are solid lines. **C**. Total tdTomato positive cells in each condition at 14 days post-infection (n=3). P values from unpaired t-test. Mean and standard deviation are plotted. **D**. Total tdTomato positive cells at the final time point for each donor, 28 or 35 days post-infection (n=3). **E**. Number of

bioRxiv preprint doi: https://doi.org/10.1101/2024.01.07.574580; this version posted January 8, 2024. The copyright holder for this preprint (which was not certified by peer review) is the author/funder, who has granted bioRxiv a license to display the preprint in perpetuity. It is made available under aCC-BY 4.0 International license.

tdTomato positive LCLs generated per condition. *Indicates conditions in which tdTomato negative LCLs were generated. **F**. EBNA-LP expression in trans-complemented LPKO LCLs and WT LCLs. W indicates number of W domains in EBNA-LP protein expressed from virus or expression construct. M indicates molecular weight marker.

Figure 2. Phosphorylation of EBNA-LP is not required for EBV-infected naïve B cell transformation. **A**. Known phosphorylated serines in EBNA-LP W domain across human EBV strains (Type 1 is B95-8, Type 2 is AG876) and EBNA-LP homologs in primate LCV strains. Identity bar indicates conservation of amino acids, with green indicating highly conserved regions, yellow indicating less conserved, and red are poorly conserved regions. Colors of residues indicate amino acid properties. Phosphorylated serines are indicated by black boxes. Previously defined conserved regions (CR1, CR2, CR3) are underlined (22). **B.** Amino acid sequence coverage of FLAG-tagged EBNA-LP (wild type) construct encoding 4 W domains expressed in 293T cells, followed by mass spectrometry of FLAG immunoprecipitation. Underlined and highlighted residues indicate peptides identified by mass spectrometry, with the number of peptides indicated below. Phosphorylated residues are red, with residue number above. **C.** Abundance of phosphorylated peptides for all identified phospho-serines out of the total peptides spanning that residue from FLAG immunoprecipitation in B. **D**. Intensity of Tandem Mass Tag (TMT) signal for peptides with S63 phosphorylation when FLAG-tagged EBNA-LP (wild type), the EBNA-LP S3A mutant, and EBNA-LP S3E mutant are expressed in 293T cells prior to FLAG immunoprecipitation, TMT labeling, and mass spectrometry (n = 3). **E**. Total tdTomato positive cells at 14 days post infection for each donor in LPKO virus infected, trans-complemented cells (n = 3). Significance determined by unpaired t-test. Mean and standard deviation are plotted. **F**. Total tdTomato positive cells at 28 or 35 days weeks post infection for each donor (n=3). **G**. Total tdTomato+ LCLs generated per condition. *Indicates conditions in which tdTomato negative LCLs were generated. **H**. Trans-complemented LPKO LCLs express wild type and mutant FLAG-tagged EBNA-LP. W indicates number of W domains in EBNA-LP protein expressed from virus or expression construct. M indicates molecular weight marker.

Figure 3. EBNA-LP contains Leucine-rich motifs which are important for adult naïve B cell transformation. **A**. Alignment of EBNA-LP W and Y domains across human EBV (Type 1 is B95-8, Type 2 is AG876) and LCV strains, with identified leucine-rich motifs highlighted in black boxes. Identity bar indicates conservation of amino acids, with green indicating highly conserved regions, yellow indicating less conserved, and red are poorly conserved regions. Colors of residues indicate amino acid properties. Previously defined conserved regions (CR1, CR2, CR3, CR4, CR5) are underlined (22). **B**. LRM Mutant construct generated with mutations in the leucine-rich domains has modified leucines to alanines. **C**. Total tdTomato positive cells at 14 days post infection for each donor in LPKO virus infected, trans-complemented cells (n = 3). **D.** Total tdTomato positive cells in adult naive B cells from three donors at 28 or 35 days post infection (n = 3). P values from unpaired t-test. Mean and standard deviation are plotted. **E.** Total tdTomato positive LCLs generated from trans-complemented LPKO infected adult naïve B cells. *Indicates conditions in which some replicates generated tdTomato negative LCLs.

Figure 4. EBNA-LP Leucine-rich motifs are important in transformation of cord blood B cells. **A**. Total tdTomato positive cells at 21 days post infection for each cord blood donor in LPKO virus infected, trans-complemented cells (n = 3). P values from unpaired t-test. Mean and standard deviation are plotted. **B.** Total tdTomato positive cells from trans-complemented cord blood B cells at 28 or 35 days post infection weeks (n = 3). **C.** Number of tdTomato positive LCLs generated from trans-complemented LPKO infected cord blood B cells. *Indicates conditions in which some replicates generated tdTomato negative LCLs. †Indicates a tdTomato negative LCL which grew out slower compared to those trans-complemented with wild type EBNA-LP.

Figure 5. EBNA-LP Leucine-rich mutant is expressed and localizes similar to wild-type EBNA-LP in LCLs derived from adult total B cell infection with LPKO virus. A. LCLs from Adult Donor 4, total B cells infected with LPKO virus retain wild type and LRM mutant EBNA-LP expression. **B**. Immunofluorescence of total B cell derived LCLs, Adult Donor 5 WT LCL, and Adult Donor 4 LPKO derived LCLs trans-complemented with wild type EBNA-LP, LRM mutant EBNA-LP, or vector only. Green = Anti-EBNA-LP (JF186), Blue = DAPI.

Figure 6. EBNA-LP associates with YY1 cellular transcription factor through leucine-rich motifs. **A.** EBNA-LP localized sites on chromatin overlap with YY1 in LCLs by publicly available ChIP-Seq data. **B**. Location on chromatin of overlapping peaks between YY1 and EBNA-LP. **C**. Endogenous co-immunoprecipitation

bioRxiv preprint doi: https://doi.org/10.1101/2024.01.07.574580; this version posted January 8, 2024. The copyright holder for this preprint (which was not certified by peer review) is the author/funder, who has granted bioRxiv a license to display the preprint in perpetuity. It is made available under aCC-BY 4.0 International license.

in LCLs to YY1. White circles indicate EBNA-LP specific bands. BJAB, an EBV-negative cell line, was used as a negative control. Signal in BJAB lanes indicate non-specific background bands. W indicates the number of W domain in the indicated isoform. **D.** FLAG-EBNALP co-immunoprecipitation in LPKO LCLs generated from trans-complementation of total B cells with vector control, wild type, or LRM mutant EBNA-LP. Signal is quantified below band. **E**. YY1 co-immunoprecipitation in trans-complemented LPKO LCLs. **F**. Relative frequency of CD46 negative cells when total B cells were transfected with Cas9/gRNA complex targeting control surface marker CD46 or CD46 and YY1 prior to infection. **G.** Relative frequency of CD46 negative naïve B cells with CD46 or CD46 and YY1 knock out prior to infection.

bioRxiv preprint doi: https://doi.org/10.1101/2024.01.07.574580; this version posted January 8, 2024. The copyright holder for this preprint (which was not certified by peer review) is the author/funder, who has granted bioRxiv a license to display the preprint in perpetuity. It is made available under aCC-BY 4.0 International license.

Supporting Information

S1 Text. Extended methods for mass spectrometry identification of EBNA-LP phosphorylation sites and quantification.

S1 Table. DNA Sequences of EBNA-LP constructs inserted into trans-complementation vector.

S1 Figure. Construction of complementation vector.
A. Plasmid map of pCEP4 vector encoding FLAG-tdTomato, followed by a P2A cleavage site, and FLAG-EBNA-LP. **B.** Amino acid sequence of EBNA-LP expressed upon P2A cleavage. FLAG tag and residues encoding EBNA-LP are underlined.

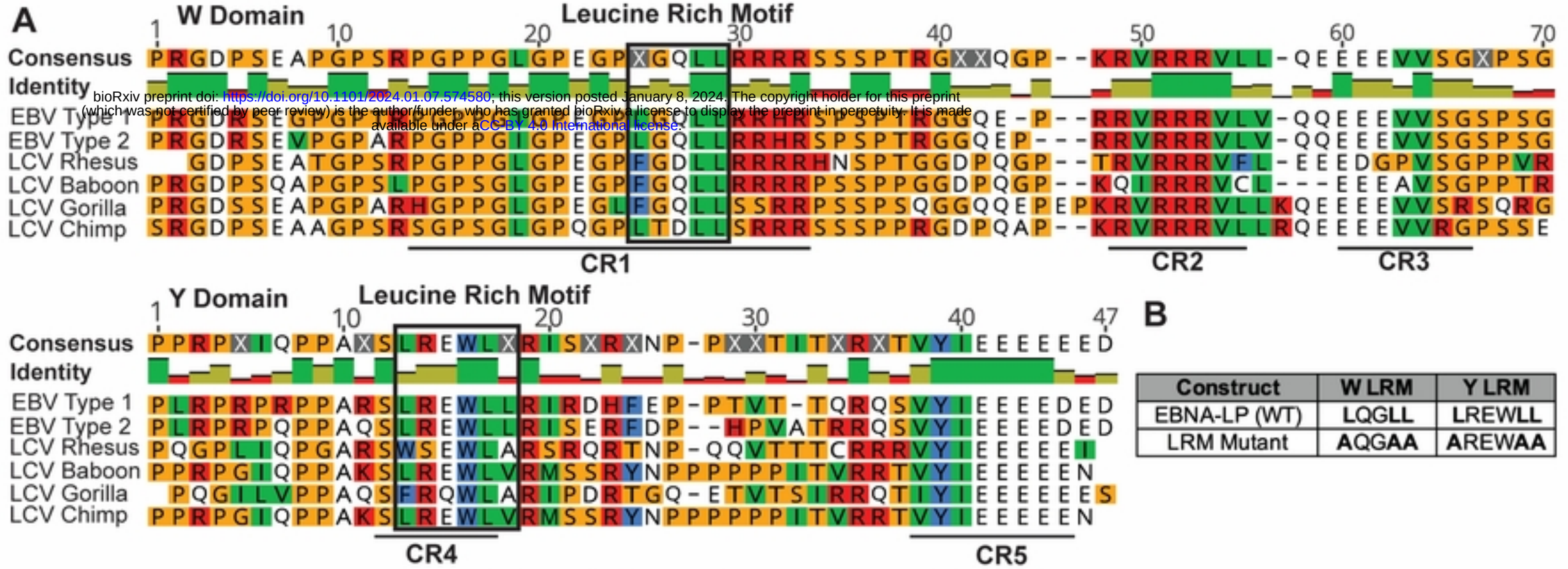
S2 Figure. Flow cytometry was used to assess tdTomato positive cells in trans-complementation assay.
A. Purity of CD19+ B cells in the naïve B cell population from adult blood donors after immunomagnetic selection prior to infection. Naïve B cells are defined as IgD+/CD27-. **B.** Gating strategy for identifying tdTomato+ cells at each time point. The virus encodes GFP, so this gating strategy is used to remove the majority of false tdTomato+ positives cells from GFP expressing cells. Representative samples from Donor 2 at 35 days post infection are shown. **C.** Total cells in each condition 14 days post infection for each donor (n=3). Mean and standard deviation are plotted. P values are determined by unpaired t-test. **D.** Total cells in each condition at 28 or 35 days post infection (n=3). **E.** In Donor 1 and Donor 3, tdTomato negative LCLs grow out in some replicates of LPKO infected untransfected cells, and LPKO infected cells transfected with control vector. Samples from Donor 3 at 35 days post infection are shown. Untransfected conditions were used to define threshold of background for tdTomato negative LCLs. Note some conditions did not lead to outgrowth of LCLs. *Indicates conditions in which cells were transformed into tdTomato negative LCLs.

S3 Figure. S34, S36, and S63 are all phosphorylated in EBNA-LP when expressed in 293T cells.
Tandem mass spectra from high-energy collisional dissocation (HCD) fragmentation localizing phosphorylation at sites S34 (**A**), S36 (**B**) and S63 (**C**) collected on a Fusion Lumos Orbitrap mass spectrometer. Localization using site-localizing y/b fragment ions were confirmed within Scaffold PTM using the AScore localization algorithm.

S4 Figure. Trans-complementation of the LPKO virus with the LRM Mutant EBNA-LP fails to generate tdTomato positive LCLs.
A. Total cells in each condition 14 days post infection for each donor (n=3). Mean and standard deviation are plotted. P values are determined by unpaired t-test. **B.** Total cells in each condition at 28 or 35 days post infection (n=3). **C.** LCLs at 35 days post infection from adult blood donors. Single cell populations are plotted for tdTomato expression at 4-5 weeks post infection. Percentage of cells that are tdTomato positive as indicated. Note that some conditions did not lead to outgrowth of LCLs. *Indicates tdTomato negative LCLs.

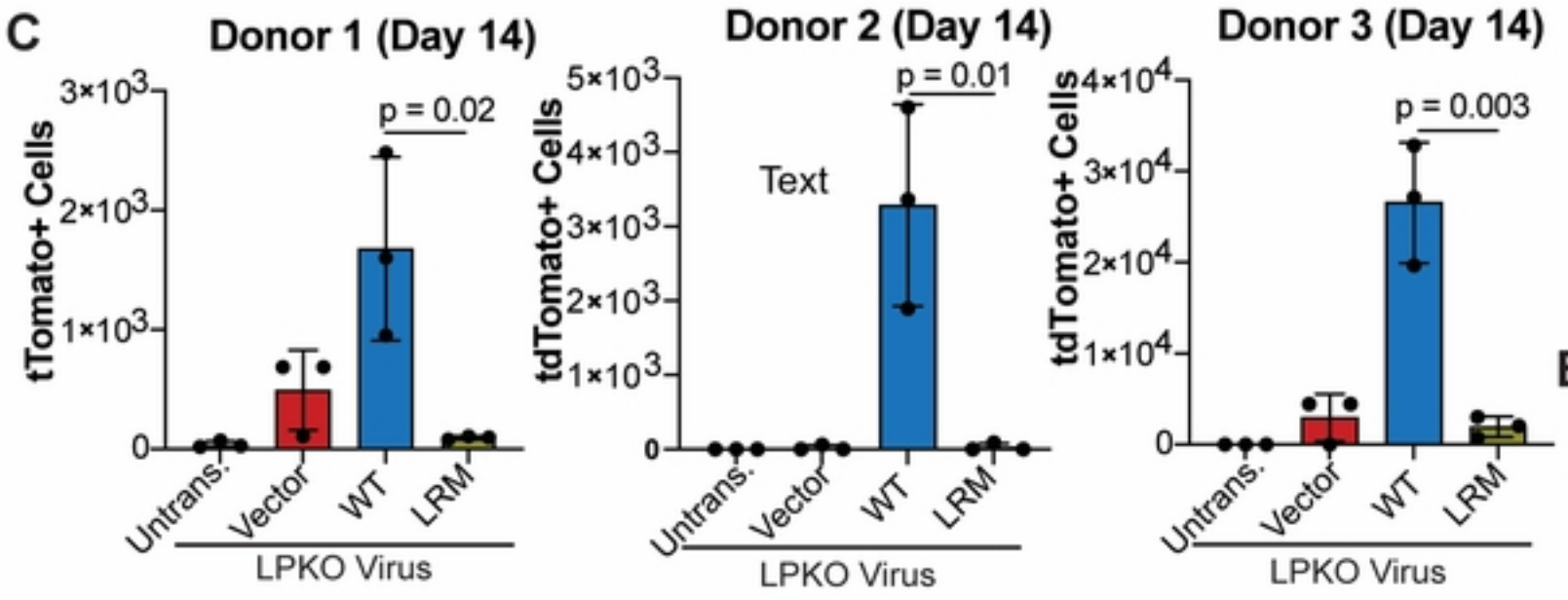
S5 Figure. Trans-complementation of LPKO infected cord blood with the EBNA-LP LRM Mutant fails to generate tdTomato positive LCLs.
A. Total cells in Cord Blood Donors in each condition 21 days post infection. Mean and standard deviation are plotted. P values determined from unpaired t-test. **B**. Total cells in Cord Blood Donors 35 days post infection. **C**. LCLs at 35 days post infection from Cord Blood Donors 1 and 2, at 5 weeks post infection. Percent indicates percent tdTomato positive cells. Note that no cells were transformed into LCLs in either donor from LPKO infected conditions that were either untransfected or transfected with control vector. *Indicates tdTomato negative LCL. **D.** Western blot of LCLs derived from cord blood donor 1.

bioRxiv preprint doi: https://doi.org/10.1101/2024.01.07.574580; this version posted January 8, 2024. The copyright holder for this preprint (which was not certified by peer review) is the author/funder, who has granted bioRxiv a license to display the preprint in perpetuity. It is made available under aCC-BY 4.0 International license.



B

Construct	W LRM	Y LRM
EBNA-LP (WT)	LQGLL	LREWLL
LRM Mutant	AQGAA	AREWAA



E

tdTomato+ LCLs	Donor 1	Donor 2	Donor 3
LPKO + Untrans.	0/3*	0/3	0/3*
LPKO + Vector	0/3*	0/3	0/3*
LPKO + WT	3/3	3/3	3/3
LPKO + LRM	0/3*	0/3*	0/3*

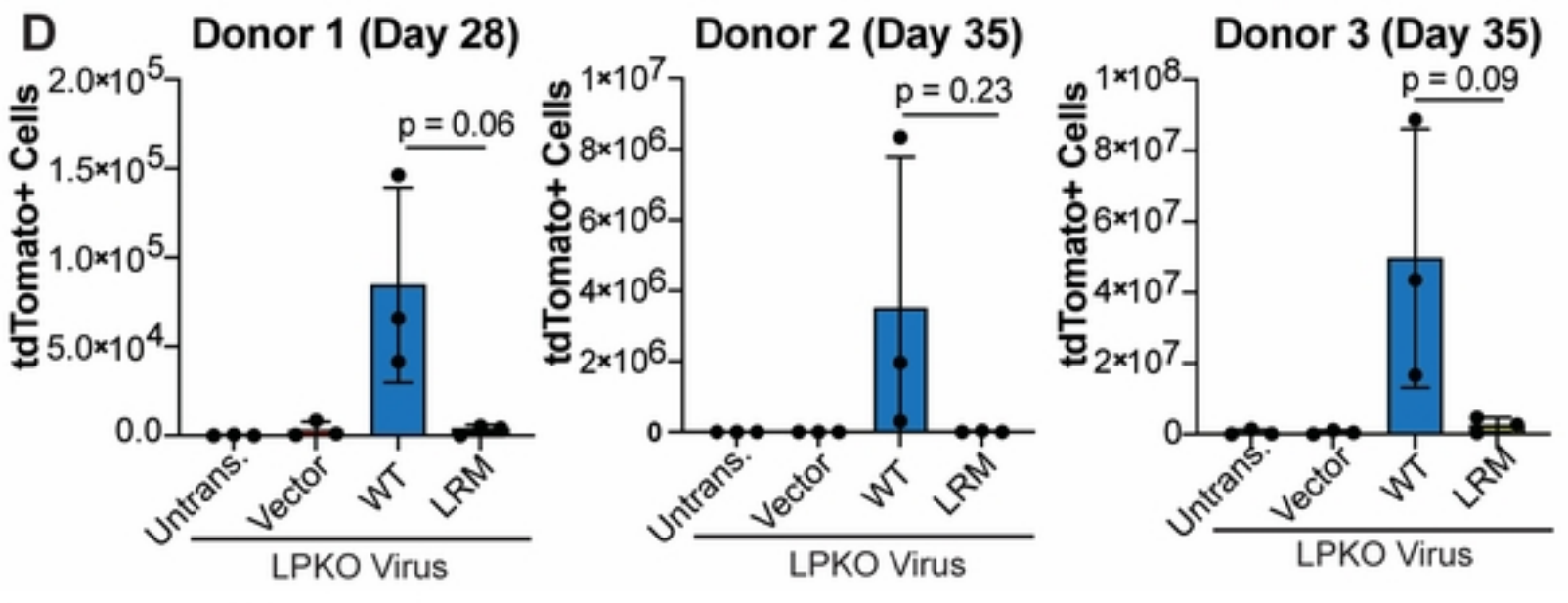
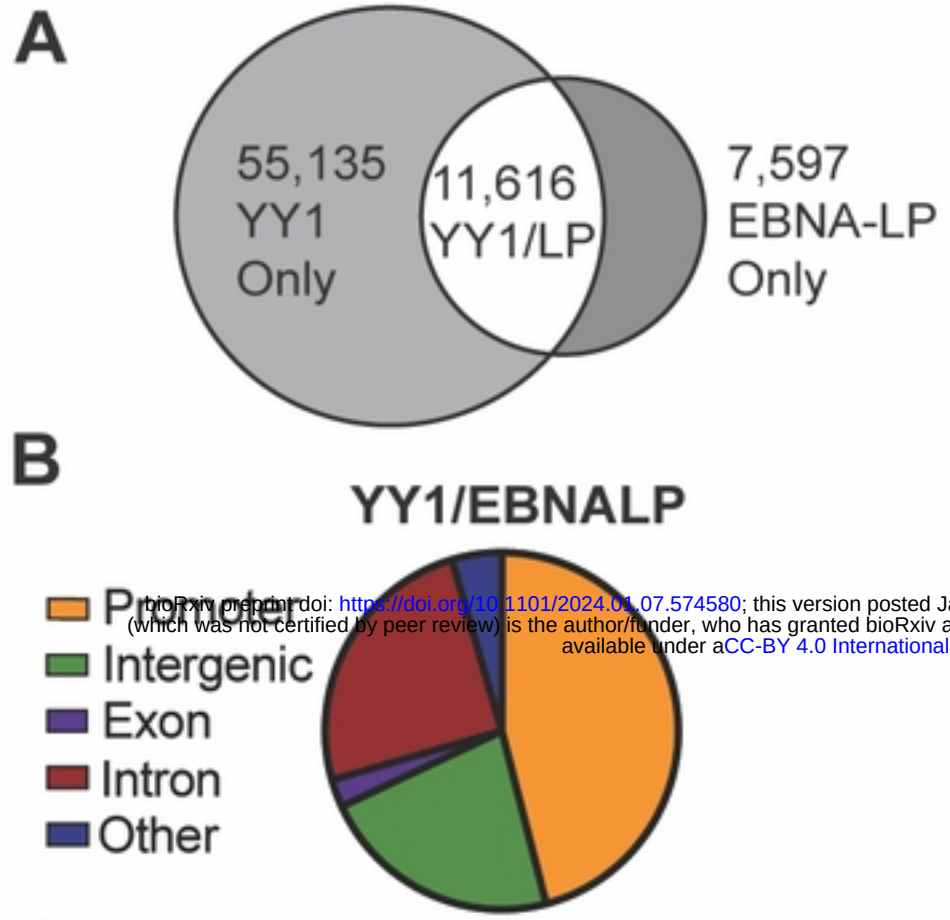


Figure 3

bioRxiv preprint doi: https://doi.org/10.1101/2024.01.07.574580; this version posted January 8, 2024. The copyright holder for this preprint (which was not certified by peer review) is the author/funder, who has granted bioRxiv a license to display the preprint in perpetuity. It is made available under aCC-BY 4.0 International license.



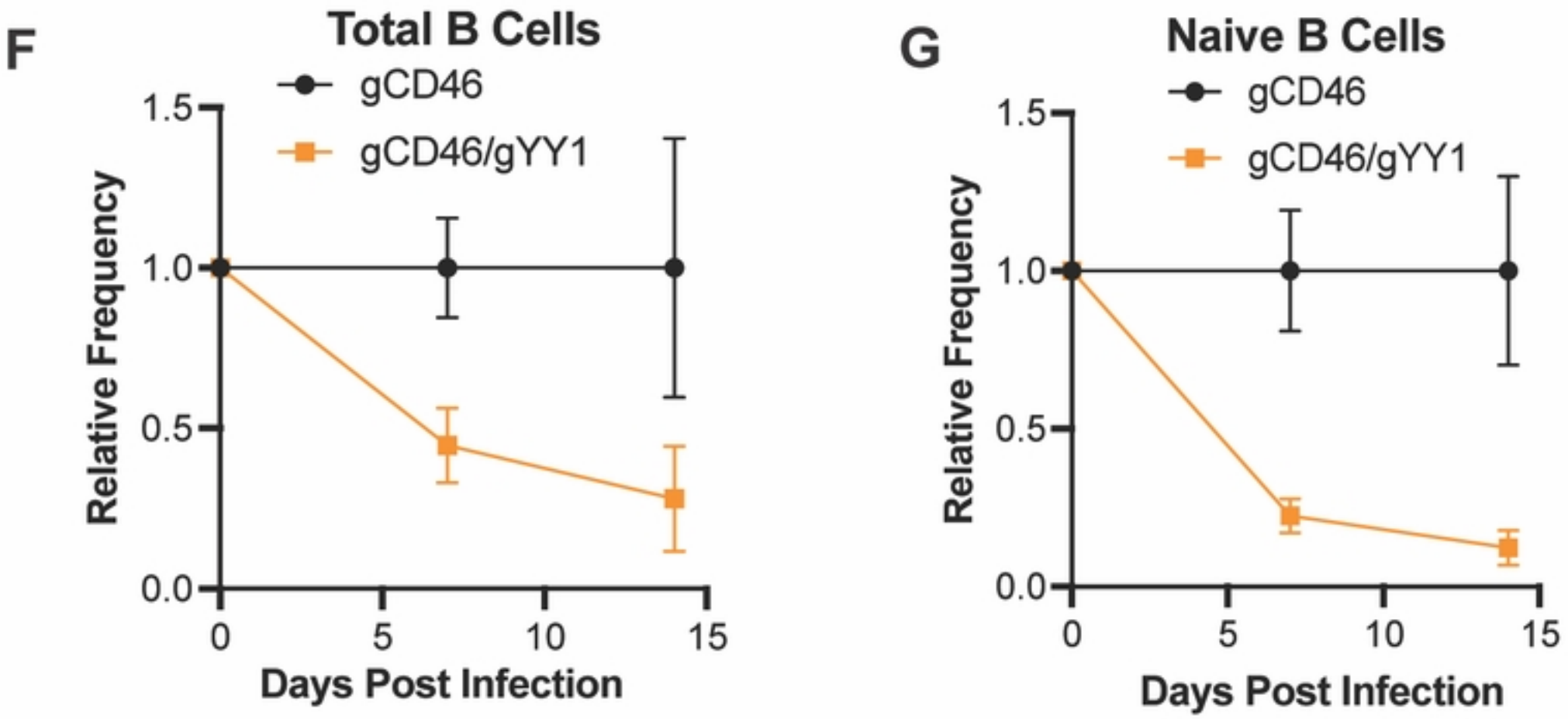
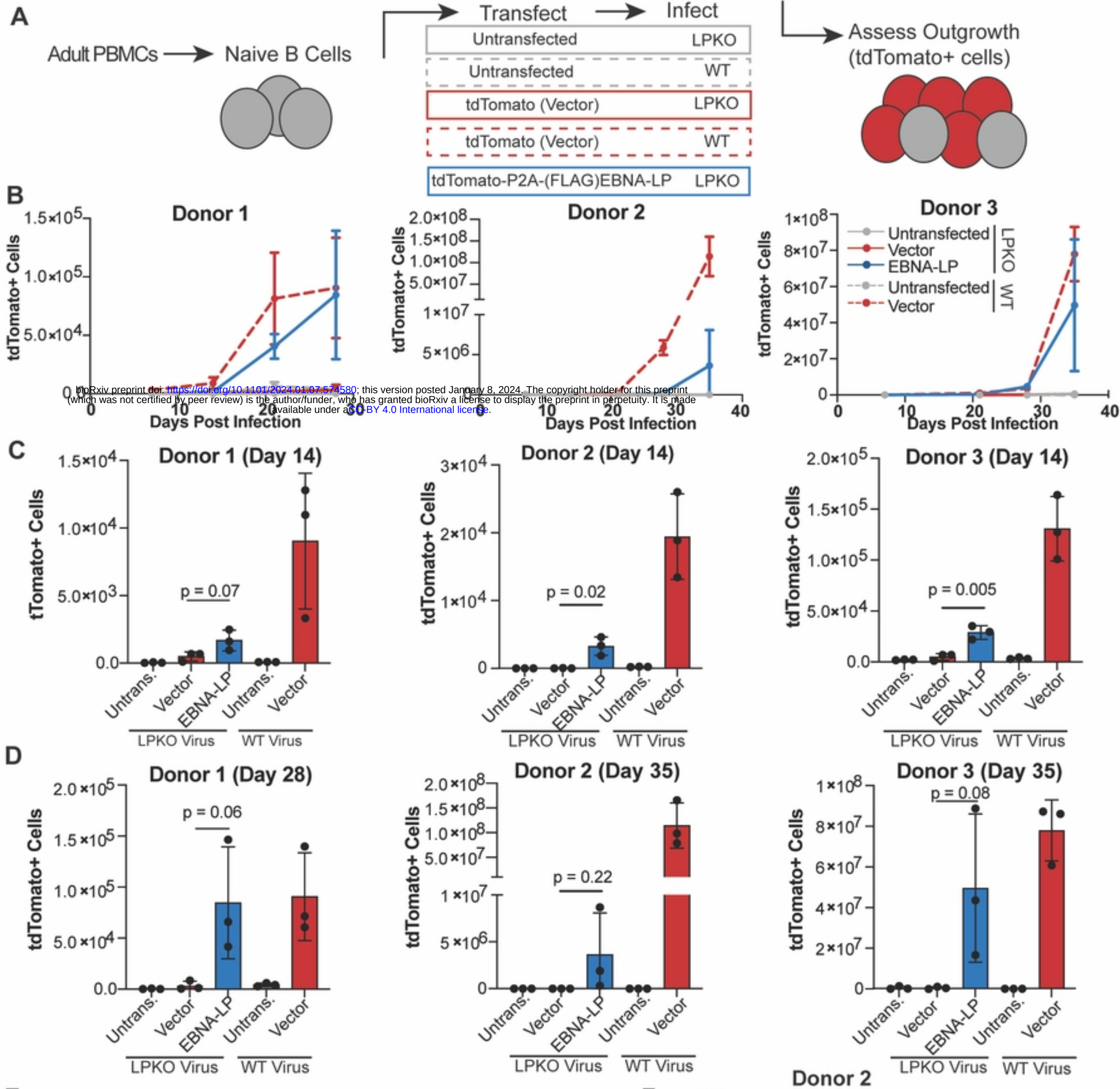


Figure 6

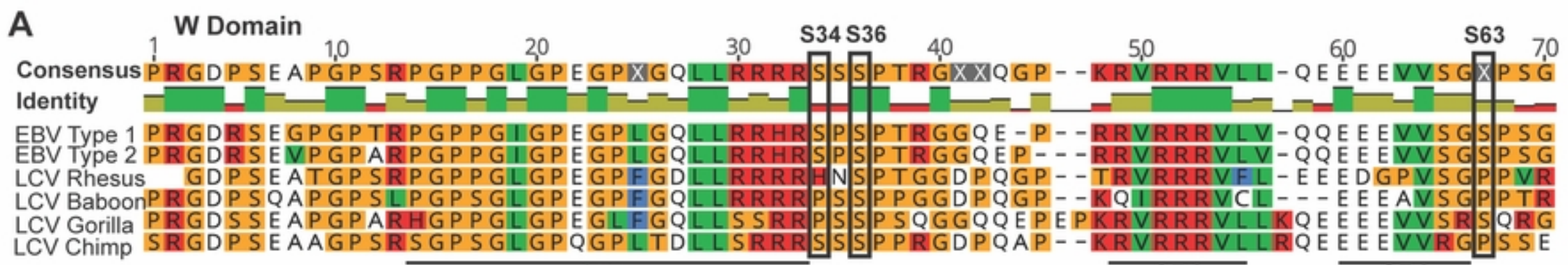
bioRxiv preprint doi: https://doi.org/10.1101/2024.01.07.574580; this version posted January 8, 2024. The copyright holder for this preprint (which was not certified by peer review) is the author/funder, who has granted bioRxiv a license to display the preprint in perpetuity. It is made available under aCC-BY 4.0 International license.



tdTomato+ LCLs	Donor 1	Donor 2	Donor 3
LPKO + Untransfected	0/3*	0/3	0/3*
LPKO + Vector	0/3*	0/3	0/3*
LPKO + EBNA-LP	3/3	3/3	3/3
WT + Untransfected	0/3*	0/3*	0/3*
WT + Vector	3/3	3/3	3/3

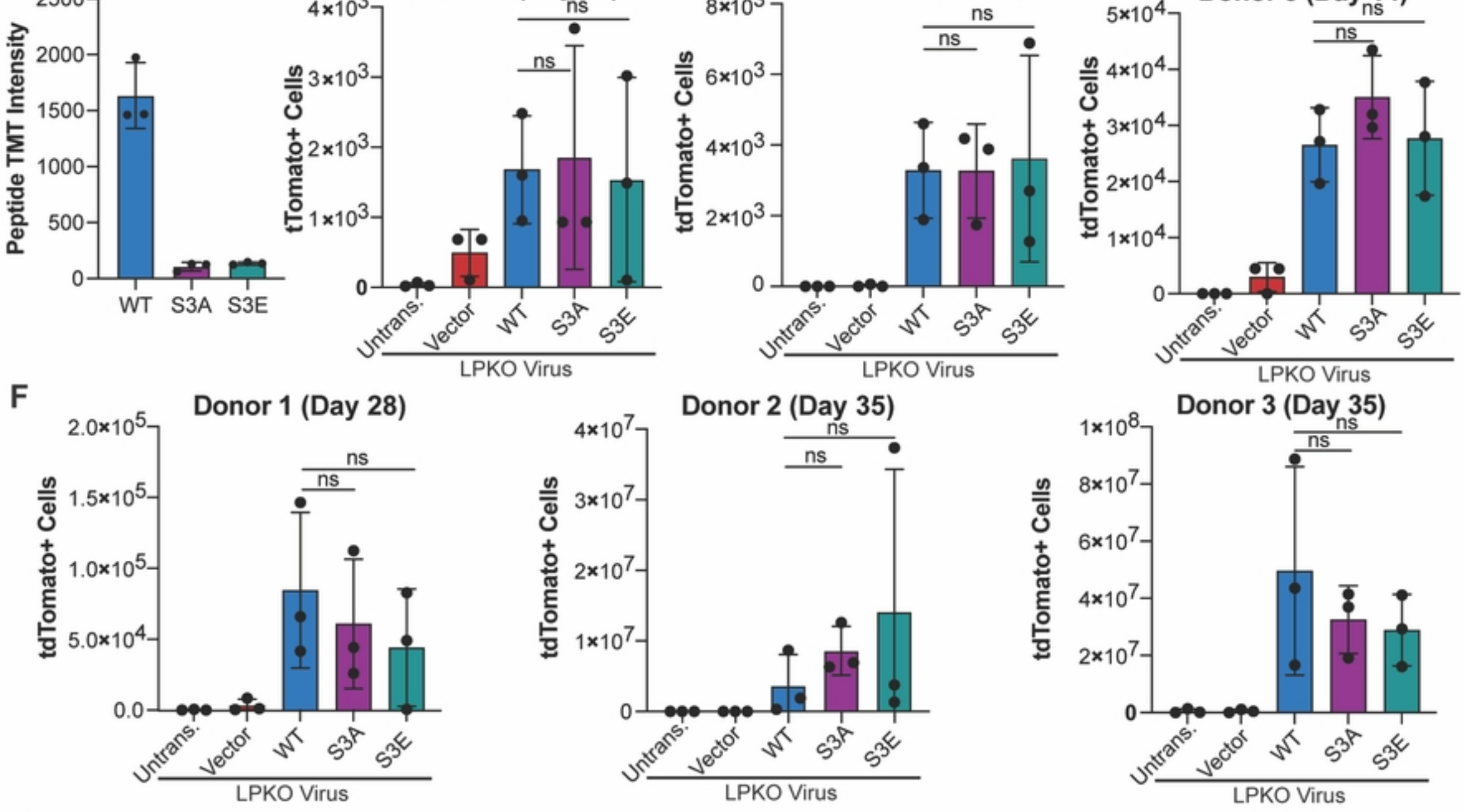
Figure 1

bioRxiv preprint doi: https://doi.org/10.1101/2024.01.07.574580; this version posted January 8, 2024. The copyright holder for this preprint (which was not certified by peer review) is the author/funder, who has granted bioRxiv a license to display the preprint in perpetuity. It is made available under aCC-BY 4.0 International license.



C

293T FLAG IP	Modification	Peptides Modified
FLAG-EBNA-LP(4)	S34 Phospho	1/2
FLAG-EBNA-LP(4)	S36 Phospho	1/2
FLAG-EBNA-LP(4)	S63 Phospho	6/41



G

tdTomato+ LCLs	Donor 1	Donor 2	Donor 3
LPKO + Untransfected	0/3*	0/3	0/3*
LPKO + Vector	0/3*	0/3	0/3*
LPKO + EBNA-LP (WT)	3/3	3/3	3/3
LPKO + S3A Mutant	3/3	3/3	3/3
LPKO + S3E Mutant	2/3	3/3	3/3

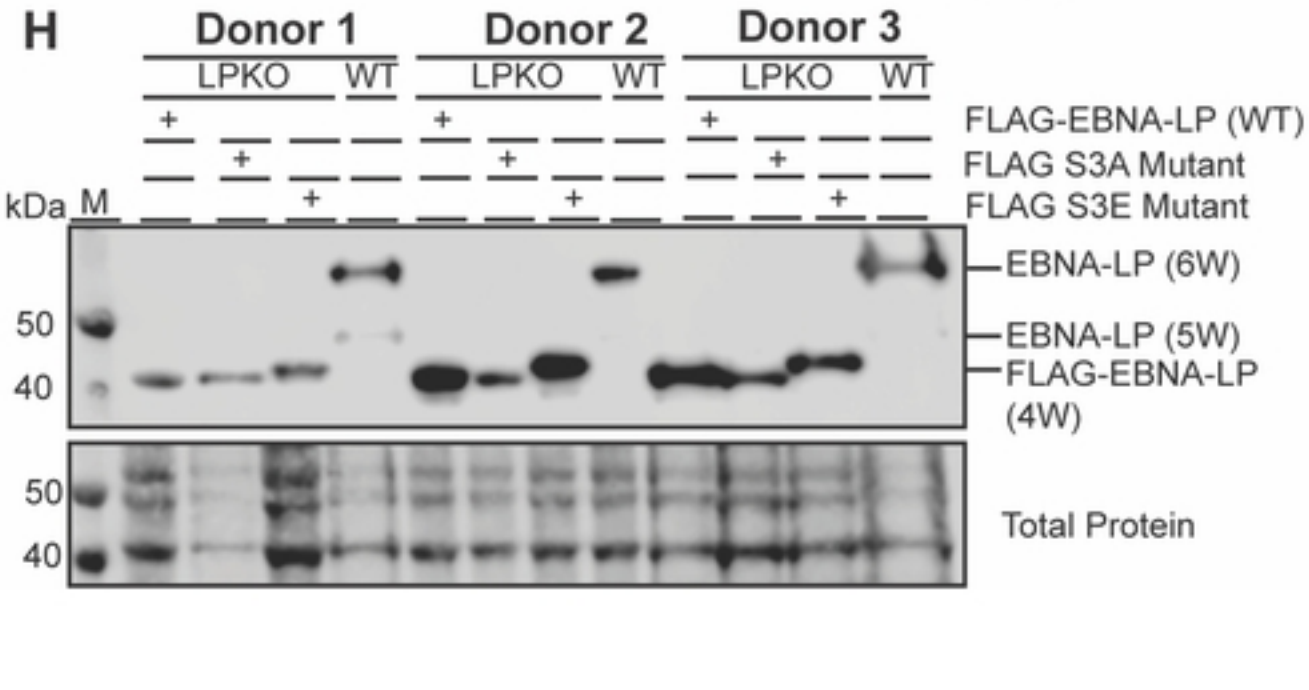
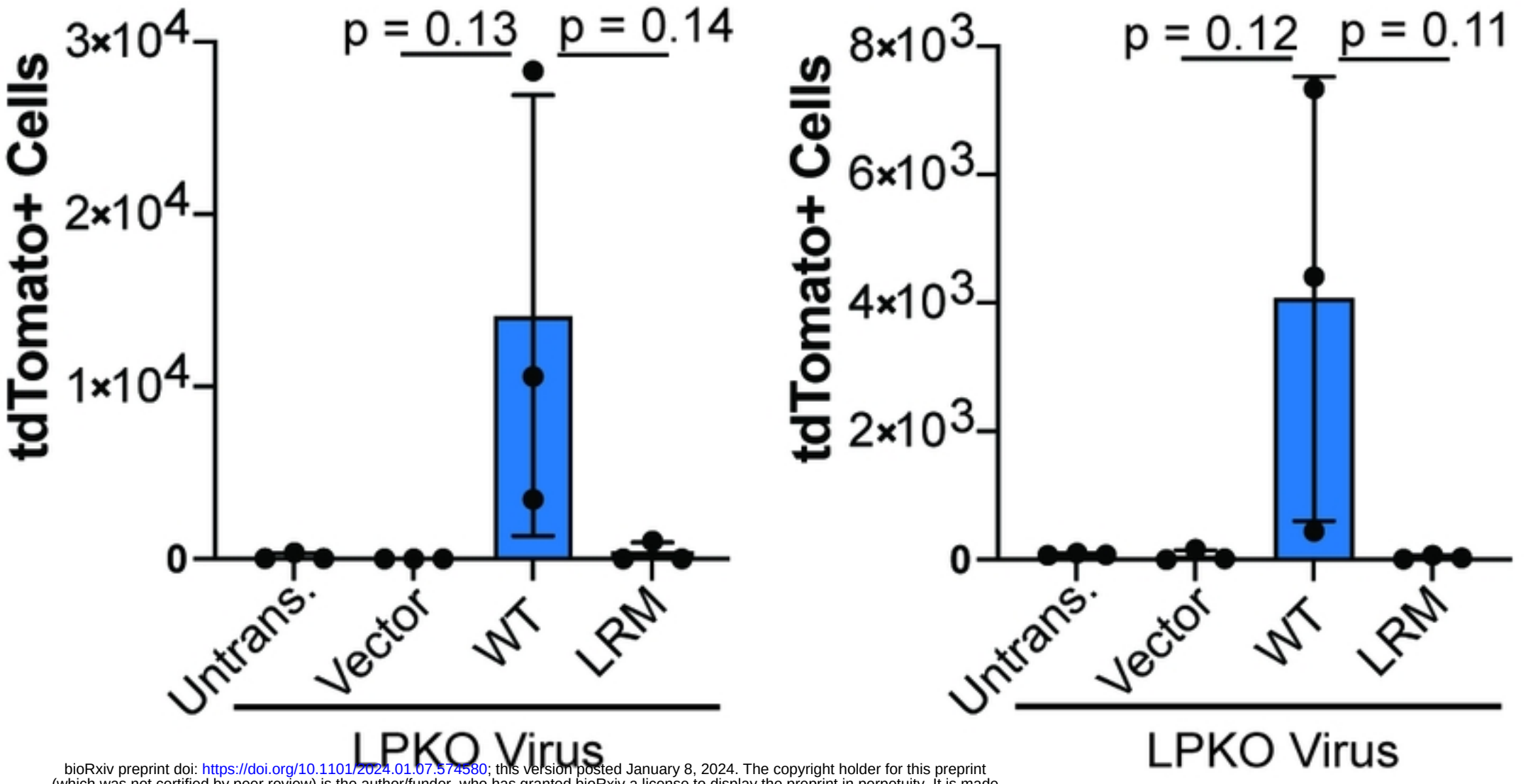


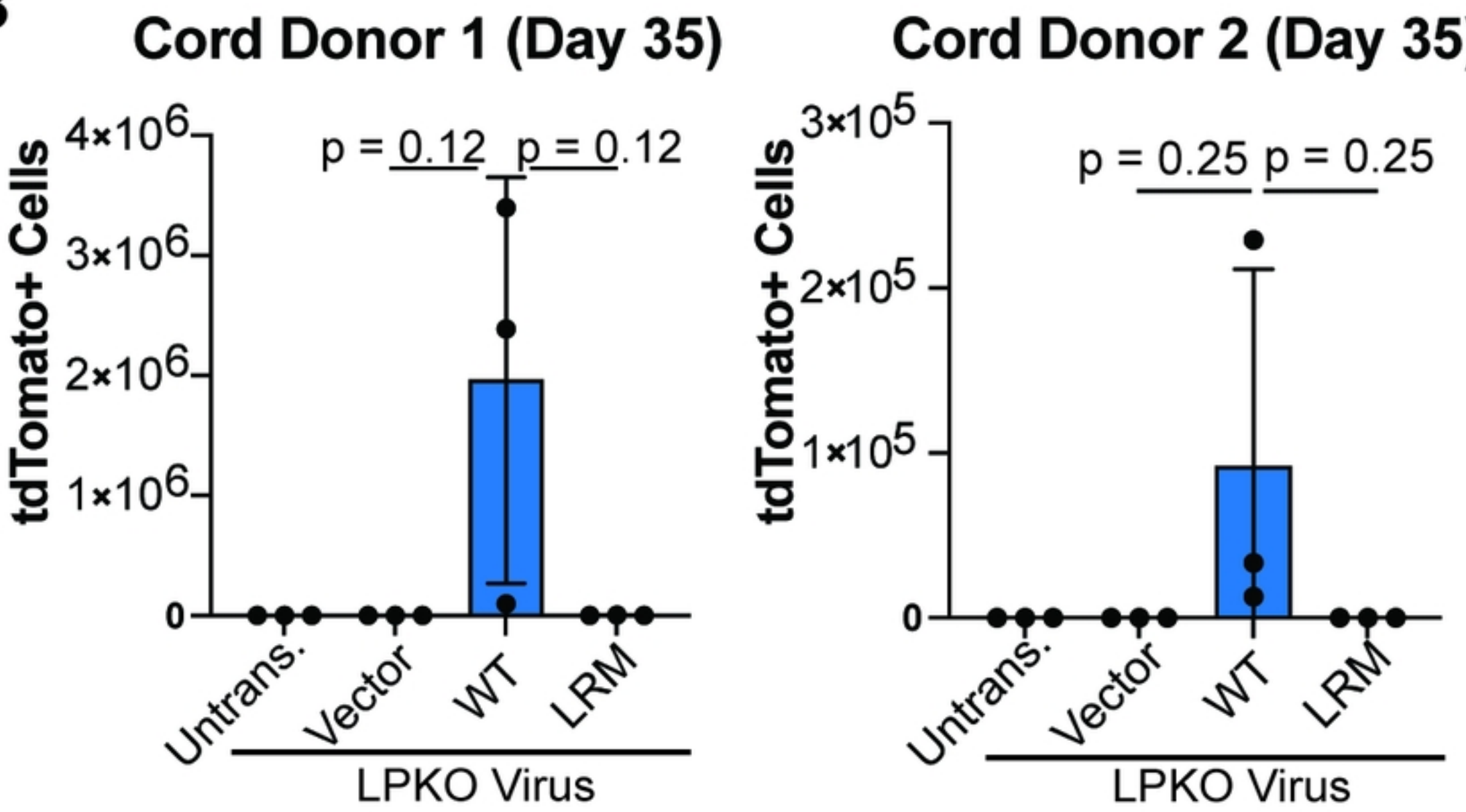
Figure 2

A



bioRxiv preprint doi: https://doi.org/10.1101/2024.01.07.574580; this version posted January 8, 2024. The copyright holder for this preprint (which was not certified by peer review) is the author/funder, who has granted bioRxiv a license to display the preprint in perpetuity. It is made available under aCC-BY 4.0 International license.

B

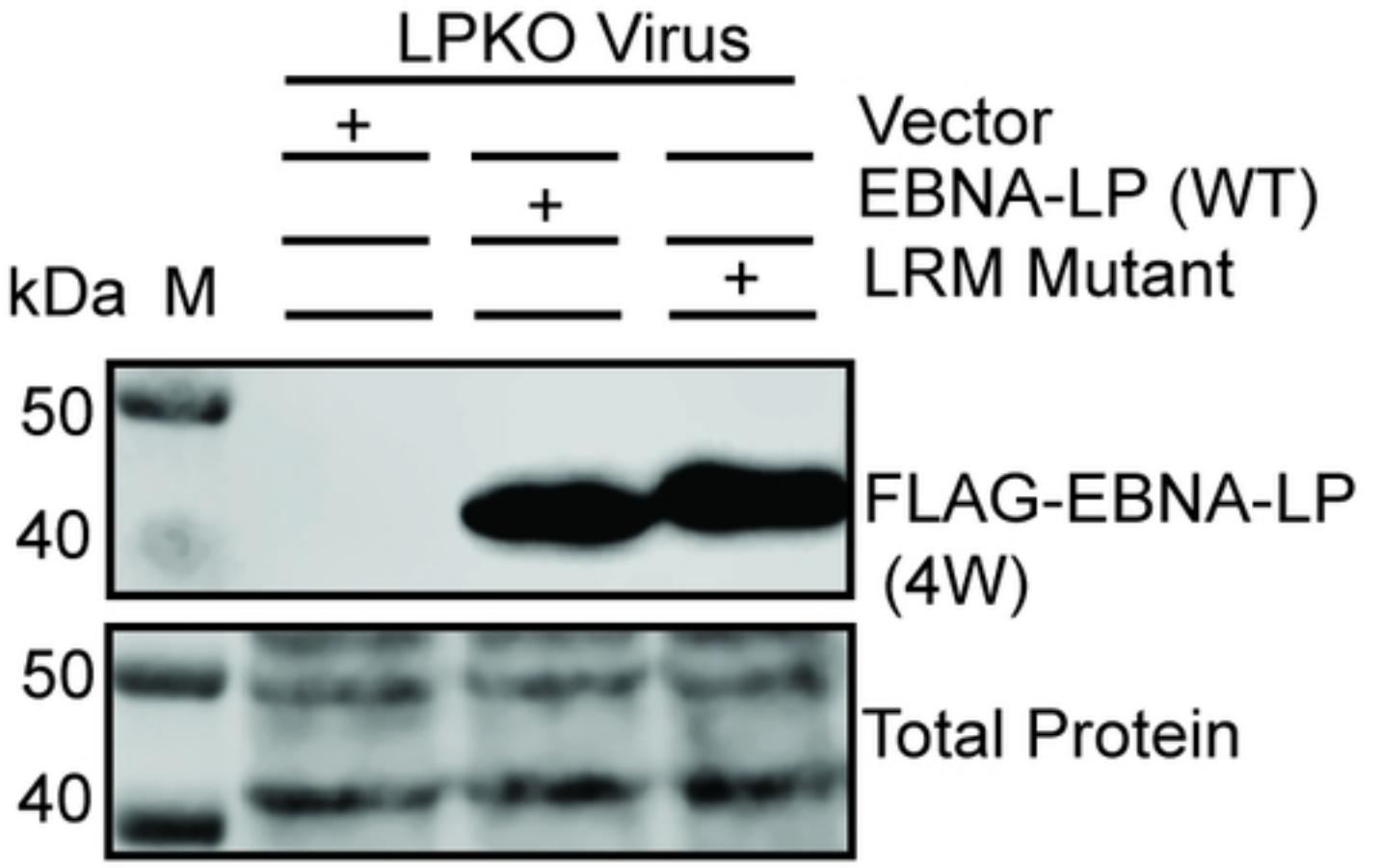


C

tdTomato+ LCLs	Cord Blood Donor 1	Cord Blood Donor 2
LPKO + Untransfected	0/3	0/3
LPKO + Vector	0/3	0/3
LPKO + EBNA-LP (WT)	3/3	3/3
LPKO + LRM Mutant	0/3*†	0/3

Figure 4

A



B

bioRxiv preprint doi: https://doi.org/10.1101/2024.01.07.574580; this version posted January 8, 2024. The copyright holder for this preprint (which was not certified by peer review) is the author/funder, who has granted bioRxiv a license to display the preprint in perpetuity. It is made available under aCC-BY 4.0 International license.

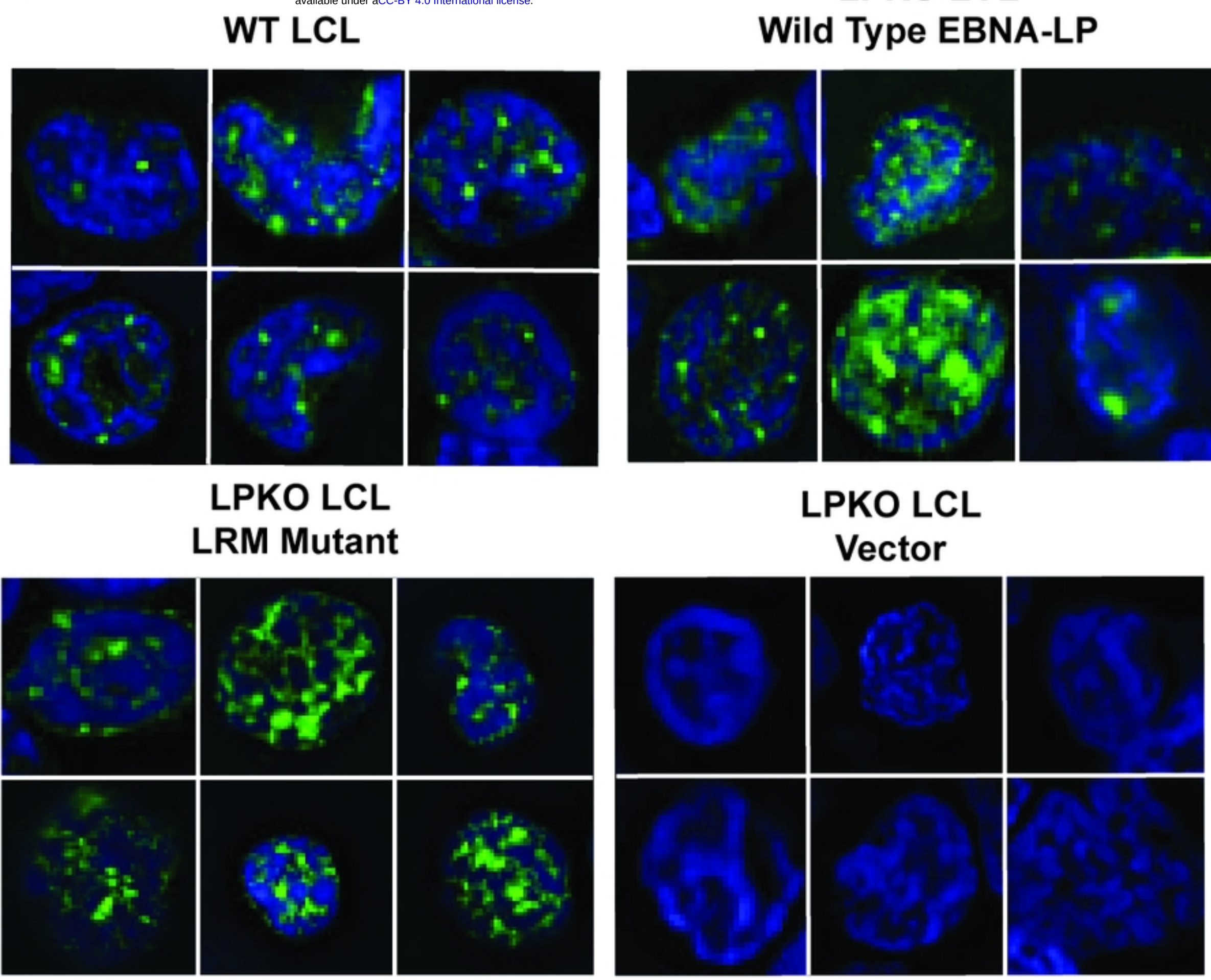


Figure 5